NATIONAL AERONAUTICS AND SPACE ADMINISTRATION

Technical Report 32-1405

Sequential Estimation of States of a Ballistic Vehicle in an Imperfectly Known Atmosphere

Antal K. Bejczy

JET PROPULSION LABORATORY
CALIFORNIA INSTITUTE OF TECHNOLOGY
PASADENA, CALIFORNIA

December 15, 1969

NATIONAL AERONAUTICS AND SPACE ADMINISTRATION

Technical Report 32-1405

Sequential Estimation of States of a Ballistic Vehicle in an Imperfectly Known Atmosphere

Antal K. Bejczy

JET PROPULSION LABORATORY
CALIFORNIA INSTITUTE OF TECHNOLOGY
PASADENA, CALIFORNIA

December 15, 1969

Prepared Under Contract No. NAS 7-100
National Aeronautics and Space Administration

Preface

The work described in this report was performed by the Guidance and Control Division of the Jet Propulsion Laboratory.

Acknowledgment

The author wishes to thank Professor R. Sridhar, Department of Electrical Engineering, California Institute of Technology, for his stimulating interest and discussions regarding the present work. The technical advice of Mr. E. H. Kopf, Jr., in using a modified DSL/90 computer simulation language, as well as the supporting interest of Mr. H. K. Bouvier and Mr. B. M. Dobrotin at JPL are gratefully acknowledged.

The present work was started at the Department of Electrical Engineering, California Institute of Technology, for JPL under NASA Contract NAS 7-100. The work was completed under a NASA-supported National Research Council Postdoctoral Resident Research Associateship at JPL.

Contents

Contents (contd)

Figures

Contents (contd)

Figures (contd)

Abstract

The *maximum principle least-squares nonlinear filter* is applied for sequentially estimating the states of a ballistic vehicle in a partially unknown atmosphere, given noisy linear or nonlinear observations on all states. Methods for reducing the filter's dimensionality and mathematical complexity are developed. An ultimate simplification of the filter scheme is obtained. Tracking performance and reliability of the simplified filter schemes are tested by extensive digital simulation studies employing the continuous formulation of the filter. The simplified filters consistently exhibit better tracking performance than the full filter schemes. Typically, the simplified filters operate with a transient time of 0.5–2.0 s.

The relative errors the simplified filters provide for the estimated states are approximately 10% or less of the relative errors in the measured states. Furthermore, the simplified filters provide reliable tracking even for 100% or more mismatch of the values of the atmospheric parameters. The ultimately simplified filter, which is a constant-gain diagonal filter, can be mechanized by approximately 95% reduction of the mathematical operations needed to mechanize the full filter.

Sequential Estimation of States of a Ballistic Vehicle in an Imperfectly Known Atmosphere

I. Introduction

A. Terminal Guidance Logic and Sequential Estimation

The basic logical functions of a guidance system designed to soft-land a vehicle on the surface of a distant planet may conveniently be organized in three major categories:

(1) *Determining* the current position and motion of the vehicle with respect to the guidance goal.

(2) *Predicting* the position and motion of the vehicle at some future time.

(3) *Deciding* what control actions are required and when to apply them in order to achieve the terminal goal.

Evidently, these operations must be performed by a logical subsystem, the essential element of which is a digital computer. The computer—accepting noisy data on the position and motion of the vehicle—then *determines* the vehicle's current state, *predicts* its future state, and *makes decisions* on necessary control actions to achieve the guidance goal.

This study is essentially concerned with the first guidance system function—that is, determining the current state of the vehicle using a digital computer as the basic tool. In particular, a ballistic vehicle flying in an imperfectly known atmosphere is considered. As a numerical example, the terminal phase of a soft-landing mission to Mars is selected.

In general, it is assumed that the current state of the vehicle would not be known with the desired accuracy for these reasons:

(1) The initial conditions for integrating the differential equations governing the vehicle's time history are known only imprecisely.

(2) The differential equations describing the vehicle's time behavior form an imperfect mathematical representation of the vehicle's true time behavior; the mathematical representation of the atmospheric forces (drag and wind) is certainly imperfect.

(3) The measurements are contaminated by inevitable noise of different origin.

Thus, a computational scheme must be developed by which the current state of the vehicle can be estimated in some optimal sense and in real-time, given (1) noisy

measurements on the state of the vehicle, and (2) an imperfect dynamic description of the time behavior of the vehicle.

Following modern concepts in the theory of estimation, the estimation procedure will be regarded as a filtering problem. Thus, the estimation logic, or scheme, is in general a dynamic time-varying multidimensional filter. The filter's input is a time sequence of noisy observations of variables related to the state. The filter uses the incoming observations in a proper way to produce up-to-date "best estimates" on the state variables by solving the equations of motion sequentially. The filter's output is then the state estimated in some optimal sense in real-time.

B. Nonlinear Filtering and the Terminal Guidance Problem

The terminal guidance problem of soft landing on an atmosphere-bearing planet involves nonlinear mathematics since (1) the state of the vehicle is governed by ordinary nonlinear *differential* equations, and (2) the measurements and the state variables are usually related to each other by nonlinear *algebraic* equations. Therefore, the nonlinear character of the terminal guidance problem should naturally lead to the application of nonlinear filtering. The conventional mathematical development of a nonlinear guidance problem, however, is based on the motions of linear perturbation techniques. These techniques allow the application of the powerful tools of linear analysis to the guidance problem. For the estimation part of the guidance problem, this would imply a possible direct application of the minimum variance (Kalman–Bucy) linear filter (Ref. 1) to producing best sequential estimates on the states of the vehicle. The application of linear perturbation techniques, however, is conditioned on an inherent requirement: the determination of a reference state. If the coordinate deviations from the reference state are outside the range of linearity, that is, if the effects of higher-order terms are not arbitrarily small anymore, the reference state has to be redetermined. Updating the reference state for improved linearizations, however, may not be feasible during the terminal phase of a planetary soft-landing mission in an atmosphere because of the partially unknown and unpredictable atmospheric conditions (atmospheric density, wind, etc.) and because of the short terminal maneuver time. The procedure of updating the reference state might eventually be eased by taking the estimated state as the reference state when it is reasonable to assume that the current best estimate is sufficiently close to the true state (Ref. 2). The application of the minimum variance linear filter to a nonlinear problem, however, remains an approximation.

In this report a *nonlinear filter* scheme is applied for estimation purposes. It is true that any hitherto known nonlinear filter is also based on approximations. The approximations involved in deriving the nonlinear filter schemes, however, are of a different mathematical significance than that of linearizing the system equations. This can easily be seen by recognizing that the known nonlinear filters (Refs. 3–9) somehow reflect upon the nonlinearities of a given problem by incorporating also the second derivatives of the system or the observation equations into the filter dynamics.

This general statement must be modified for the nonlinear filter derived by Cox (Ref. 3). This filter is essentially equivalent to using linear filtering about the computed mean, or, alternatively, it is equivalent to the minimum variance filter for a linear expansion of the system's nonlinearities. The known computational studies on the performance of *nonlinear* filters indicate (Ref. 10) that any nonlinear filter has a better response for the nonlinear estimation problems than a strictly linear one.

Among the known nonlinear filters, the maximum principle least-squares (MPLS) nonlinear filter (Ref. 4) is employed in this study for estimating the states of a ballistic vehicle flying in a partially unknown atmospheric environment. The particularly appealing feature of the MPLS nonlinear filter is the filter's deterministic derivation which does not require the specification or computation of quantitative probabilities. The satisfactory performance of the MPLS nonlinear filter is merely based upon a judicious choice of the relative weightings for the residual errors.

The MPLS nonlinear filter, as compared to the other known nonlinear filters, introduces the second derivatives only of the *observation* equations into the filter's dynamics, leaving the second derivatives of the *system* equations out of the filter scheme. For the problem under consideration, this yields a simpler filter structure as well as a more proper estimation scheme than any other known nonlinear filter would give. The estimation scheme provided by the MPLS nonlinear filter is "more proper" for the problem under consideration in the sense that the observations necessarily should have more relative importance in the estimation scheme than the system equations because of the imperfect knowledge on the acting atmospheric forces (drag, wind, etc.).

C. Purpose and Approach

During the terminal phase of a soft-landing mission to a distant planet the possibility of earth-vehicle communication is excluded. This necessitates that the logical operations of the terminal guidance system must rely entirely upon vehicleborne measurements and vehicleborne data analysis. It is required, therefore, that all terminal guidance functions be accomplished by on-board self-contained equipment. This basic requirement also implies that the computations related to the logical operations of the terminal guidance system must not be too complex to be executed by a special-purpose on-board computer having limited weight and computation capacity. The particular objective of this study regarding the development of a realizable sequential estimation scheme is motivated by that practical constraint. Thus, this report is essentially a study on well-defined and useful simplifications of the MPLS nonlinear filter scheme applied to sequentially estimating the states of a ballistic vehicle flying in a partially unknown planetary atmosphere.

To test the feasibility of the derived simplified MPLS nonlinear filter scheme, extensive numerical experimentations were carried out on a digital computer. The ultimate justification for the approximations and simplifications employed in the present study is essentially based on digital simulations. Theoretical considerations are used only for motivating the simplifications and for substantiating the obtained results.

The performance of realizable nonlinear filters can ultimately be judged probably only by application, as it is also indicated by several other researchers on nonlinear filtering (Ref. 11). Therefore, the application itself also enters into the analysis and design of the nonlinear filter. This implies that the approximations and simplifications applied in the present study should primarily be viewed in relation to the particular problem in question. Nevertheless, these simplifications and the related results may be indicative regarding other particular problems, too.

II. The Maximum Principle Least-Squares Nonlinear Filter

The MPLS filter is derived (Ref. 4) using deterministic techniques. Thus, no probabilistic assumptions or computations are required regarding the measurement errors and the unknown inputs to the system. This fact is of considerable importance since in many cases the determination of valid statistical data on the acting disturbances is in itself a difficult theoretical and practical problem. For estimation purposes, the minimization of the integral of the weighted squared residual errors (estimation errors) is used.[1] The sequential nature of the estimation problem is brought out by applying the theory of invariant imbedding on the canonical equations formally obtained using the Pontryagin maximum principle. The derived MPLS nonlinear filter equations are first-order approximations to a nonlinear partial differential equation resulting from the invariant imbedding[2].

A. Nonlinear Filter Equations

For quick reference the general MPLS nonlinear filter equations are summarized below in a convenient form.

$$\frac{d}{dT}\hat{x} = f(\hat{x},T) + P(T)g(\hat{x},T) \tag{1}$$

$$\frac{d}{dT}P = F(\hat{x},T)P(T) + P(T)\overline{F}(\hat{x},T) + P(T)G(\hat{x},T)P(T) + R \tag{2}$$

$$g(\hat{x},T) = 2\,\overline{H}(\hat{x},T)Q[y(T) - h(\hat{x},T)] \tag{3}$$

where

T = running estimation time

$\hat{x}$ = best estimate of the n-dimensional state vector (*best* in the least-squares sense)

$f(\hat{x},T)$ = n-vector function; system equations in form of first-order ordinary differential equations for the state vector x with respect to time t.

$F(\hat{x},T) = \left(\frac{\partial f_i}{\partial x_j}\right)$ = the Jacobian function matrix of f

$\overline{F}$ = the transpose of F

$h(\hat{x},T)$ = m-vector function; the observation vector relating the measurement vector $y(T)$ to the state vector $\hat{x}$; $m \leqslant n$

$\overline{H}(\hat{x},T) = \left(\overline{\frac{\partial h_i}{\partial \hat{x}_j}}\right)$ = the transpose of the Jacobian function matrix of h

[1]It has to be noted that the application of the least-squares criterion for estimation purposes will not necessarily be the best one if valid statistical data on the acting disturbances are at hand.

[2]As a matter of fact, this nonlinear partial differential equation can also be obtained immediately using the dynamic programming approach.

$G(\hat{x},T) = \left(\frac{\partial g_i}{\partial \hat{x}_j}\right)$ = the Jacobian function matrix of g

Q = quasi-norm factor; positive semi-definite $m \cdot m$ symmetric matrix related to the observation vector

$R = \frac{1}{2}W^{-1}$ = the inverse of the matrix W

W = quasi-norm factor; positive definite $n \cdot n$ symmetric matrix related to the system equations

P = $n \cdot n$ symmetric matrix; gain matrix; (approximate covariance matrix)

The dynamic structure of the MPLS nonlinear filter, in the form of a functional flow diagram, is shown in Fig. 1.

A close inspection of the structure of Eqs. (1–3) reveals that the sequential estimation of states through the MPLS nonlinear filter scheme is, in effect, accomplished by fitting solutions of the equations of motion to the measured data in a weighted least-squares sense. Furthermore, the following features have to be noted regarding the MPLS nonlinear filter scheme.

B. General Features of the Filter Equations

(1) This scheme contains $n(n+3)/2$ coupled, ordinary nonlinear differential equations where n is the dimensionality of the system.

(2) The state estimator equations, Eq. (1), are in proper form since, if the current observation should happen to agree precisely with the estimated observable, the fact that observation took place would have no effect on the rate of change of the estimate.

(3) In general, the observations y_i appear as forcing terms in the state estimator equations as well as in the gain equations. Furthermore, the gain equations will also contain the second derivative of the observation vector h.

(4) When the observation vector h is a linear one, the gain equations will not contain the observations y_i as forcing terms since there is no second derivative of the observation vector. The gain equations read then

$$\frac{d}{dT}P = F\,P + P\,\overline{F} - 2P\,\overline{H}\,Q\,H\,P + R \qquad (4)$$

(5) The relative weightings, Q and W (or R), for the residual errors must be specified. Assigning relative weights replaces the requirement of specifying the mean and covariance of the noise terms when a probabilistic approach is employed.

(6) When solving or implementing the differential equations of the MPLS nonlinear filter scheme, initial values must be assigned for $\hat{x}$ and P. It has to be noted also that P must be a positive definite matrix.

C. Digital Simulation of the Filter

In general, there is no way to investigate the tracking performance and stability of the MPLS nonlinear filter other than by simulation studies for given cases or for given class of cases. The procedure of digital simulation of the MPLS nonlinear filter is schematically depicted in Fig. 2. Thus, the digital simulation of this filter contains the following phases:

(1) The trajectories of the dynamically perturbed system are generated by solving the system equations for given initial conditions.

(2) Noisy observations are generated by corrupting the output data of phase 1 with suitably modeled observation noise.

(3) The noisy observations, generated through phase 2, are used as input to the relevant MPLS nonlinear filter equations which then have to be solved for assumed initial values for $\hat{x}$ and P and with selected values for the weighting matrices Q and R.

The main problems in studying the behavior of the MPLS nonlinear filter are to determine the appropriate weighting matrices Q and R as well as to determine the proper initiation for integrating the filter equations. In general, these problems must be solved by trial and error using the following obvious criteria as guides to evaluate the estimated trajectories. The estimated trajectories must have simultaneously:

(1) Short transient parts toward the true trajectories.

(2) Smooth and stable behavior along the true trajectories.

(3) Insensitivity for a given class of wrong initial estimates on the states and for a given class of perturbations.

The numerical algorithms employed in the digital simulations must also be accounted for in a proper way

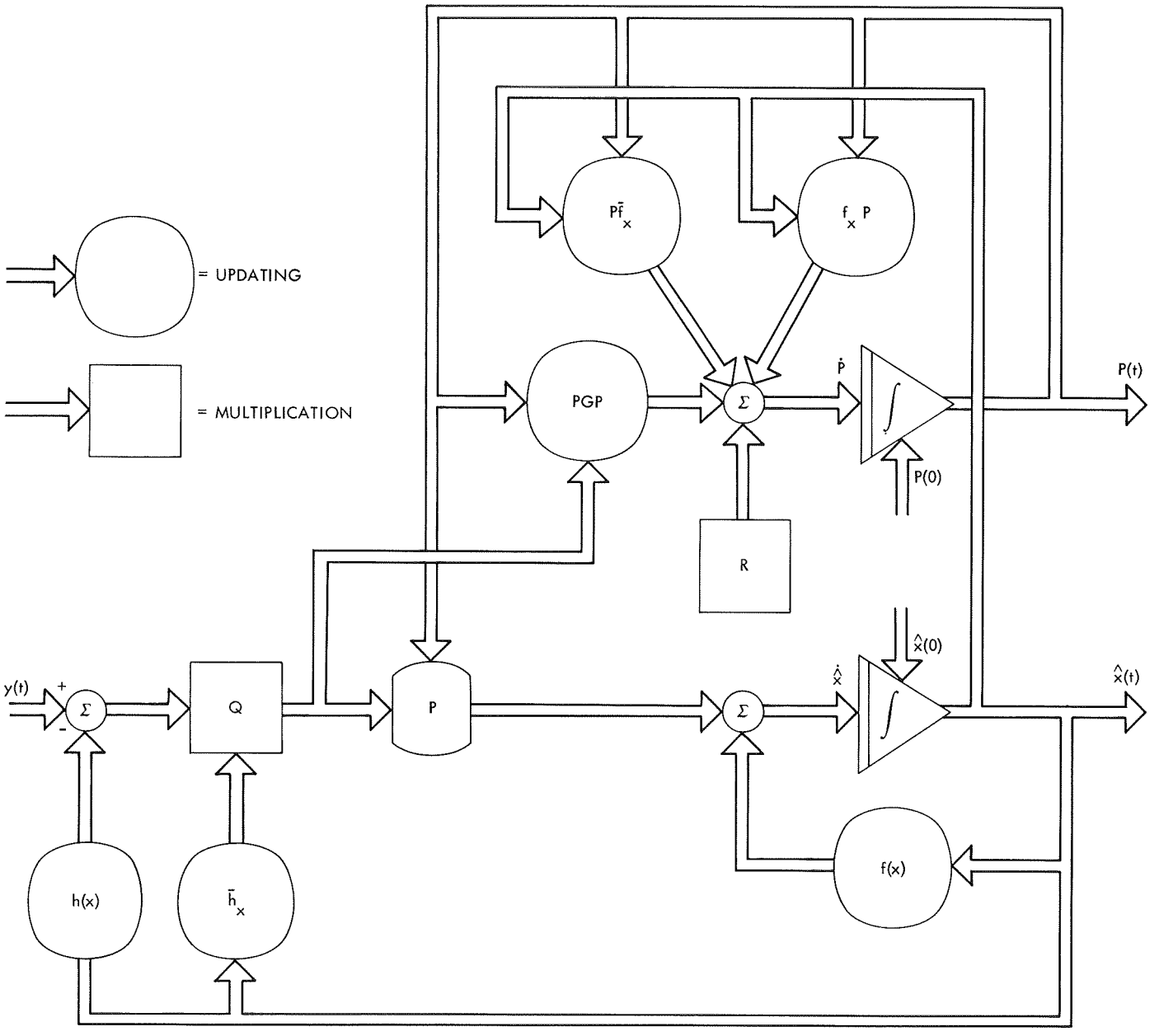

Fig. 1. Functional flow diagram for the maximum principle least-squares nonlinear filter

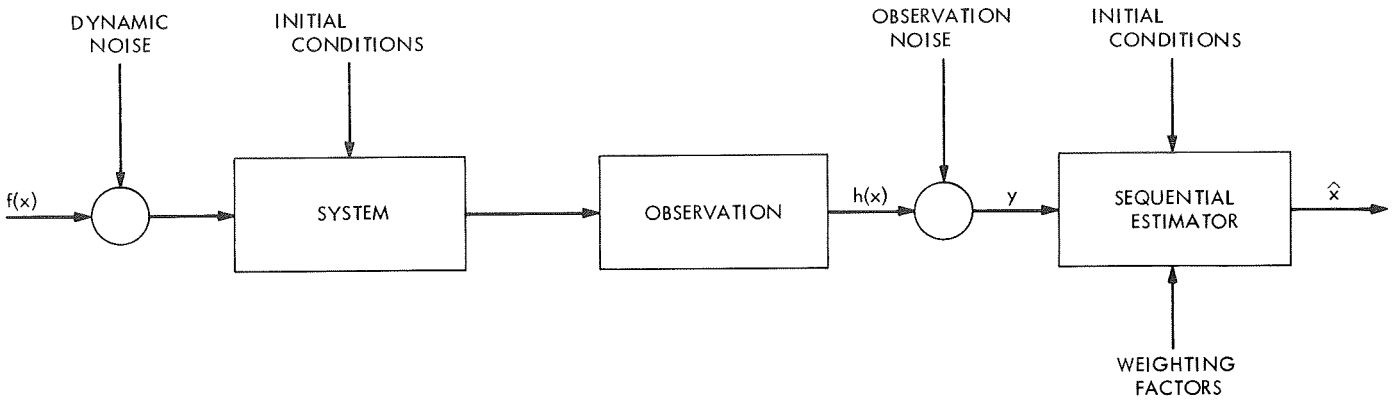

Fig. 2. Scheme of digital simulation of the filter equations

when studying the tracking performance and stability of the MPLS nonlinear filter in its continuous formulation. The numerical algorithms do necessarily interfere with the tracking performance and stability of any nonlinear filter.

III. Simplifications of the Maximum Principle Least-Squares Nonlinear Filter Dynamics

When dealing with sequential estimation of states of multivariable nonlinear systems, the gain equations of the MPLS nonlinear filter—depending on the dynamic description and on the dimensionality of the system—attain an increasingly complex *Riccati* structure. From a solution and mechanization point of view, therefore, it may be imperative to simplify the dynamics of the full MPLS nonlinear filter in a well-defined manner. (Note that the full MPLS nonlinear filter scheme itself is but an approximation.)

A. Propositions

The following propositions are set forth (Ref. 12) for simplifying the dynamics of the MPLS nonlinear filter scheme.

(1) *Proposition 1:* All but the diagonal gain equations in the MPLS nonlinear filter should be disregarded when all state variables are available for measurement.

(2) *Proposition 2:* If the diagonal gain equations of the MPLS nonlinear filter settle down on constant values, these values should be applied as constant gains in the diagonally reduced filter from the initiation of sequential estimation, thus omitting the on-line solution or mechanization of all gain equations in the filter.

Proposition 1 may be justified heuristically by adopting an information-transmission point of view regarding the structure of the MPLS nonlinear filter scheme. The diagonal gain equations transmit direct contributions from the measurements to estimating the state vector. Direct contribution means, for instance, the contribution from velocity measurements to estimating velocity. On the other hand, the off-diagonal gain equations transmit indirect or cross-correlated contributions from the measurements to estimating the state vector. Indirect contribution means the contribution from velocity measurements to estimating position or, inversely, the contribution from position measurements to estimating velocity.

It is worthwhile to note that the contribution from velocity measurements to estimating position, and the contribution from position measurements to estimating velocity, may be transmitted by the same gain term because of the symmetry of the gain matrix.

Taking into account these structural characteristics of the MPLS nonlinear filter, it may be true that the full filter operates in a physically and mathematically redundant manner. But this information-transmission point of view on the filter's structure, as briefly outlined above, warrants further investigation.

B. Consequences

Proposition 1 implies that

$$\frac{d}{dt}P_{ij} \equiv P_{ij} \equiv 0 \text{ for } i,j = 1,2,\cdots,n, i \neq j \qquad (5)$$

when the proposed diagonal time-varying filter scheme is employed to estimate the state vector. The approximation given by Eq. (5) amounts to choosing the off-diagonal elements of the weighting matrix R (or W)

formally in the following way:

$$R_{ij} + \sum_{i=1}^{n} a_{ji} P_{ii} \equiv 0 \qquad (6)$$

where the terms a_{ji} are the relevant elements of the Jacobians. The computations involved in Eq. (6) need not be performed to get an operating diagonal time-varying filter. The specification of Eq. (6) is merely a formal one. Nevertheless, it is necessary to specify Eq. (6) formally to get balance in the off-diagonal gain equations which, in general, also contain the diagonal elements of the gain matrix. At the same time, Eq. (6) also provides insight into the simplifications afforded by proposition 1. In view of Eq. (6), the role of the R_{ii} terms in the simplified diagonal gain equations may also be reinterpreted. Thus, the R_{ii} terms tend also to compensate for the cancelled off-diagonal terms in the simplified diagonal gain equations.

Proposition 1 introduces considerable mathematical simplifications into the structure of the full MPLS nonlinear filter scheme. First, the dimensionality of the filter is being reduced to $2n$ from the original $n(n+3)/2$ dimensions. Moreover, the dynamics of the remaining filter equations are being simplified, too, because the number of terms has been reduced in each remaining filter equation.

Proposition 2 yields the following simplified MPLS nonlinear filter scheme:

$$\frac{d}{dT}\hat{\hat{x}} = f(\hat{\hat{x}},T) + 2P^*\bar{H}\,Q\,[y(T) - h(\hat{\hat{x}})] \qquad (7)$$

The symbols used in Eq. (7) are defined as in Section II-A (except for P^* which is a constant, diagonal $n \cdot n$ matrix, the elements of which are the settled-down values of the diagonal P equations in the corresponding diagonally reduced filter).

The dynamic structure of the constant-gain diagonal filter is shown in Fig. 3. Comparison of Figs. 3 and 1 will aid in understanding the operational simplifications associated with the constant-gain diagonal filter scheme.

The motivation for proposition 2 and for the resulting diagonal constant gain filter is the existence of the settled-down values of the diagonal P equations in the diagonally reduced filter.

It should be noted that Eq. (7) represents the ultimate simplifying reduction of the MPLS nonlinear filter scheme. The dimensionality of this diagonal constant-gain filter is n, which is the same as the dimensionality of the system in question. Moreover, in this ultimately simplified MPLS nonlinear filter scheme there is only one term which is being added to each system equation. These additional single terms alone will take care of the running observations when Eq. (7) is solved sequentially to estimate the current value of the state vector.

The ultimate justification for the simplifications of the MPLS nonlinear filter defined by propositions 1 and 2 must be based on numerical studies of given problems. The subsequent sections of this document are devoted to numerical studies on the tracking performance and stability of the simplified MPLS nonlinear filters as applied to sequential estimation of states of a ballistic vehicle flying in an imperfectly known atmosphere.

C. Free Manipulations in the Simulation Procedure

The formal procedure of digital simulation of the simplified MPLS nonlinear filters—the diagonal time-varying and the diagonal constant-gain filters—is the same as that outlined previously for the full filter, depicted in Fig. 2.

In general, there are three elements which can be chosen freely (but judiciously) when studying the tracking performance and stability of the simplified (as well as of the full) filters through digital simulation: (1) the initial conditions for $\hat{\hat{x}}$ and P, (2) the noise model and unknown inputs, and (3) the weighting matrices. These three independent free accesses to the digitally simulated filters are separately emphasized in Fig. 2.

IV. Time-Varying Diagonal Filter

The system equations describing the drag-retarded planar motion of a gravity-turn ballistic vehicle at the terminal phase of a soft-landing mission are derived in Appendix A. The vehicle is considered to be still in free fall; that is, no retrothrust is applied for braking. A linear and a nonlinear observation vector related to the vehicle's motion are also specified in Appendix A. In specifying the observation vectors and deriving the MPLS nonlinear filter equations, it has been assumed that the sequential estimation problem is restricted to estimating altitude,

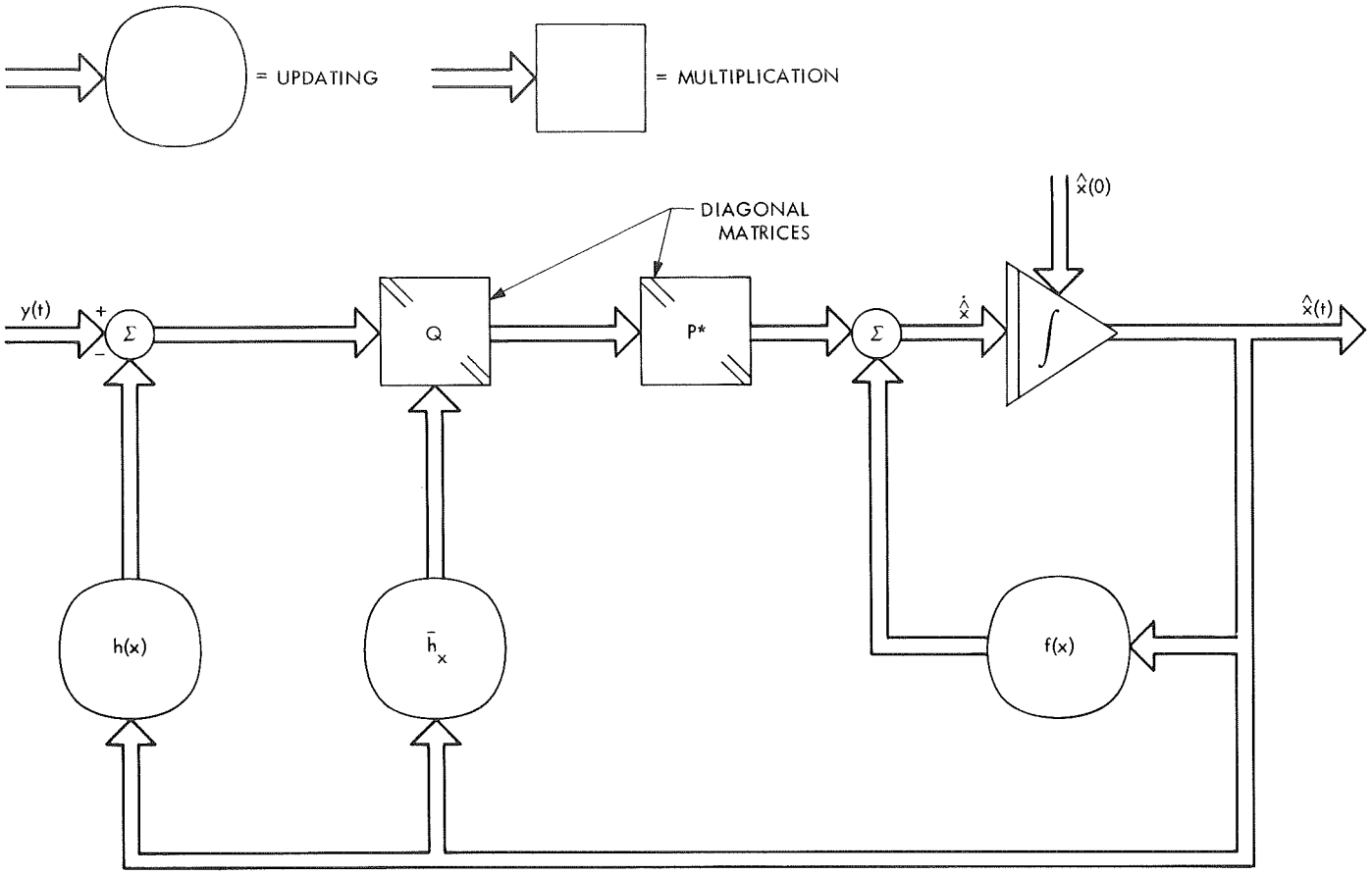

Fig. 3. Functional flow diagram for the maximum principle least-squares constant-gain diagonal nonlinear filter

path angle, and velocity—the essential system variables from the point of view of the terminal guidance goal. The observation vectors are selected such that their dimensionality is the same as that of the state vector to be estimated (that is, all state variables are measured).

The full MPLS nonlinear filter equations for the specified linear and nonlinear observation vectors are derived in Appendixes B and C, respectively. The main difference between the two sets of filter equations is the role of observations in the gain differential equations (the $\dot{P}_{ij}$ equations). The observations appear as forcing terms in the $\dot{P}_{ij}$ equations for the nonlinear observations, while, in the case of the linear observations they appear as forcing terms only in $\dot{\hat{x}}_i$ (estimated mean) equations (and not at all in the $\dot{P}_{ij}$ equations).

The gain differential equations, however, are dependent on the estimated mean of the states in both cases. This implies that the gain differential equations of the MPLS nonlinear filter scheme must be solved simultaneously with the state estimator equations.[3] The initial conditions on the filter equations and the elements of the R matrix must be specified when solving Eqs. (B-4) through (B-12) (Appendix B) and Eqs. (C-4) through (C-12) (Appendix C), respectively. The tracking performance and stability of the MPLS nonlinear filter depend mainly on the judicious choice of the initial conditions and of the R matrix, as noted previously.

The solutions of the full MPLS nonlinear filter equations for estimating altitude, path angle, and velocity are not presented here for each simulated case since the aim of this report is the study of the solutions of the simplified MPLS filter schemes as they are specified in the previous section.

[3]This is in sharp contrast to the solution of the minimum variance linear (Kalman–Bucy) filter equations where the gains can be precomputed.

A. Linear Observations

According to proposition 1, defined by Eqs. (5) and (6), the time-varying diagonally reduced filter equations for sequentially estimating altitude, path angle, and velocity, given noisy linear observations on all states, become [from Eqs. (B-4) through (B-12) in Appendix B]:

$$\dot{\hat{x}}_1 = -\hat{x}_3 \sin \hat{x}_2 + 2P_{11}(y_1 - \hat{x}_1) \tag{8}$$

$$\dot{\hat{x}}_2 = \left(\frac{g}{\hat{x}_3} - \frac{\hat{x}_3}{r}\right) \cos \hat{x}_2 + 2P_{22}(y_2 - \hat{x}_2) \tag{9}$$

$$\dot{\hat{x}}_3 = g \sin \hat{x}_2 - K\hat{x}_3^2 \exp(-b\hat{x}_1) + 2P_{33}(y_3 - \hat{x}_3) \tag{10}$$

$$\dot{P}_{11} = -2P_{11}^2 + \bar{R}_{11} \tag{11}$$

$$\dot{P}_{22} = -2P_{22}^2 - 2P_{22} \sin \hat{x}_2 \left(\frac{g}{\hat{x}_3} - \frac{\hat{x}_3}{r}\right) + \bar{R}_{22} \tag{12}$$

$$\dot{P}_{33} = -2P_{33}^2 - 4P_{33} K\hat{x}_3 \exp(-b\hat{x}_1) + \bar{R}_{33} \tag{13}$$

Comparing Eqs. (8–13) to those in Appendix B (B-4 through B-12), it is seen that the time-varying diagonally reduced filter scheme has a much simpler structure than the full filter scheme. The new features of the time-varying diagonally reduced filter equations as compared to the full filter equations are the following:

(1) The filter scheme's dimensionality is reduced from nine to six.

(2) The terms in the diagonal filter equations are reduced by a factor of two.

(3) The diagonal gain differential equations are decoupled from each other.

(4) There is only one gain term in each state estimator equation, Eqs. (8–10), which takes care of the running observations.

(5) The state-dependent coefficients of the linear terms in Eqs. (12) and (13) essentially are the second and third diagonal elements of the Jacobian of the system equations. [Note that the first diagonal element of that Jacobian, given by Eq. (B-3) of Appendix B, is zero; consequently, there is no linear term in the first gain equation, Eq. (11).]

(6) The meaning of the diagonal elements of the weighting matrix R is reinterpreted in the diagonally reduced filter scheme (signified by a superior horizontal bar: $\bar{R}_{ii}$).

1. Input data. In the digital simulation of the time-varying diagonal filter, given by Eqs. (8–13), the following $\bar{R}_{ii}$ values were applied:

$$\bar{R}_{11} = 1, \bar{R}_{22} = 5, \bar{R}_{33} = 50$$
$$\bar{R}_{11} = 5, \bar{R}_{22} = 10, \bar{R}_{33} = 75$$
$$\bar{R}_{11} = 10, \bar{R}_{22} = 15, \bar{R}_{33} = 100$$

The initial conditions on P_{ii} were

$$P_{11}(0) = P_{22}(0) = P_{33}(0) = 0$$

The estimated initial values of the state variables were 20–40% off to the "true" values. Typical true initial values were:

$$x_1(0) = 1.5\text{–}2.0 \times 10^4 \text{ ft}$$
$$x_2(0) = 50\text{–}60 \text{ deg}$$
$$x_3(0) = 6.0\text{–}9.0 \times 10^2 \text{ ft/s}$$

Dynamic noise and observation noise were modeled according to the expression

$$n_i = a_i \eta_i(t) \tag{14}$$

where $\eta_i(t)$ are, for each t, statistically independent random variables, uniformly distributed between $[+1, -1]$ and a_i are constants, adjusted to the assumed relative magnitude of the respective noise. In generating noise the following relative amplitudes were assumed:

(1) 10–30% dynamic noise.

(2) 0.5–2.0% noise in altitude measurements.

(3) 2.0–8.0% noise in path angle measurements.

(4) 1.0–6.0% noise in velocity measurements.

The fourth-order Runge–Kutta routine was employed for integrating the filter differential equations. The integration step size was 0.01 s. The physical parameters applied in the computations as well as the applied computer subroutines are listed in Appendix D.

2. General results. The main results of the digital simulations of the time-varying diagonal filter for linear observations can be summarized as follows.

a. Tracking performance and stability. In general, the tracking performance and stability of the simplified filter

equations are very good. A typical case is shown in the curves of Fig. 4 for a selected set of $\overline{R}_{ii}$. After a very short transient time ($\approx$1.0 s), the simplified filter tracks the true trajectories smoothly. The amplitude of the low-frequency oscillations of the estimated trajectories around the true trajectories is less than 10% of the relative amplitude of the measurement noise.

b. Initiation of the filtering process. The response of the simplified filter to the wrong initial conditions on the state variables is very satisfactory. As is clearly displayed in Fig. 4, the filter's tracking performance is very much insensitive to the wrong initial estimates on the states.

c. R_{ii} value comparison. The *high* $\overline{R}_{ii}$ values result in shorter transient parts for the estimated trajectories than the *low* $\overline{R}_{ii}$ values, while the low $\overline{R}_{ii}$ values yield smoother estimated trajectories than the high $\overline{R}_{ii}$ values.

d. Constant gains. The gain equations of the simplified filter scheme settle to some constant values after a short transient time. The values of these settled constants, shown in the curves of Fig. 5, depend strongly on the selected values of $\overline{R}_{ii}$, but are not dependent on the initial conditions on P_{ii}. The very fact that the different P_{ii} gains, for identical values of $\overline{R}_{ii}$, settle to almost the same constant values shows that the linear terms in the simplified gain equations have a relatively insignificant role. In this connection, it should be remembered that the coefficients of these linear terms are the corresponding derivatives of the system equations.

e. Reliability. The reliability of the simplified filter regarding its tracking performance and stability remains unchanged when applying it in different regions of the state space for sequentially estimating the state vector.

f. Tracking performance. The simplified filter has faster and smoother tracking performance than the full filter scheme. The apparent reason for this is that the cross-correlated contributions from the observation vector to estimating the state variables have a retarding effect on the convergence of the component equations of the full filter scheme.

3. Comparison of the full and simplified filters. For the sake of simplicity, the simulation of a vertical trajectory is quoted here to illustrate the tracking performance and dynamics of the full filter as compared to the tracking performance and dynamics of the diagonally reduced filter.

The full MPLS filter scheme for sequentially estimating altitude and velocity in vertical descent, given linear observations on altitude and velocity, is given by the following differential equations[4]:

$$\dot{\hat{x}}_1 = -\hat{x}_3 + 2P_{11}(y_1 - \hat{x}_1) + 2P_{13}(y_3 - \hat{x}_3) \tag{15}$$

$$\dot{\hat{x}}_3 = g - K\hat{x}_3^2 \exp(-b\hat{x}_1) + 2P_{13}(y_1 - \hat{x}_1) + 2P_{33}(y_3 - \hat{x}_3) \tag{16}$$

$$\dot{P}_{11} = -2P_{13} - 2(P_{11}^2 + P_{13}^2) + R_{11} \tag{17}$$

$$\dot{P}_{13} = -P_{33} + Kb\hat{x}_3^2 \exp(-b\hat{x}_1)P_{11} - 2K\hat{x}_2 \exp(-b\hat{x}_1)P_{13} - 2(P_{11}P_{13} + P_{33}P_{13}) + R_{13} \tag{18}$$

$$\dot{P}_{33} = 2Kb\hat{x}_3^2 \exp(-b\hat{x}_1)P_{13} - 4K\hat{x}_3 \exp(-b\hat{x}_1)P_{33} - 2(P_{13}^2 + P_{33}^2) + R_{33} \tag{19}$$

According to proposition 1 defined by Eqs. (5) and (6), putting $\dot{P}_{13} = P_{13} = 0$ in Eqs. (15–19), the simplified time-varying diagonal filter for sequentially estimating altitude and velocity of a vertically descending vehicle then becomes:

$$\dot{\hat{x}}_1 = -\hat{x}_3 + 2P_{11}(y_1 - \hat{x}_1) \tag{20}$$

$$\dot{\hat{x}}_3 = g - K\hat{x}_3^2 \exp(-b\hat{x}_1) + 2P_{33}(y_3 - \hat{x}_3) \tag{21}$$

$$\dot{P}_{11} = -2P_{11}^2 + \overline{R}_{11} \tag{22}$$

$$\dot{P}_{33} = -4K\hat{x}_3 \exp(-b\hat{x}_1)P_{33} - 2P_{33}^2 + \overline{R}_{33} \tag{23}$$

In simulating the full as well as the simplified filters for the vertical case, given by Eqs. (15–23), the same noise and initial conditions were applied as for the ballistic case described previously. The obtained results are shown in Fig. 6.

The curves of Fig. 6 clearly show that the simplified, diagonally reduced filter has a better tracking performance than the full filter. For the sake of uniformity in comparing the tracking performance of the diagonal filter to that of the full filter, the results shown in Fig. 6 were obtained with the same R_{11} and R_{33} values for both filters and with $R_{13} = 0$ for the full filter.

[4]These equations can be obtained from Eqs. (B-4) through (B-12) in Appendix B by omitting the equations for $\dot{\hat{x}}_2$, $\dot{P}_{12}$, $\dot{P}_{22}$, $\dot{P}_{23}$ and putting $P_{12} = P_{22} = P_{23} = 0$ and $\hat{x}_2 = \pi/2$ in the remaining equations.

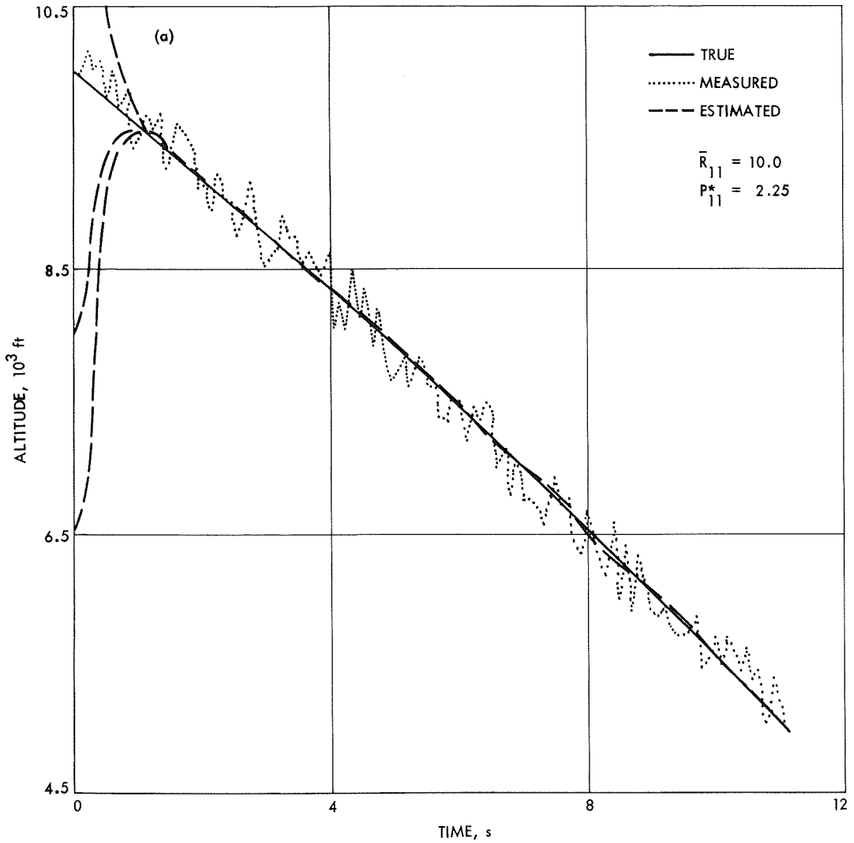
(a)
TRUE
MEASURED
ESTIMATED
$\bar{R}_{11}$ = 10.0
P^*_{11} = 2.25
ALTITUDE, 10^3 ft
10.5
8.5
6.5
4.5
0
4
8
12
TIME, s

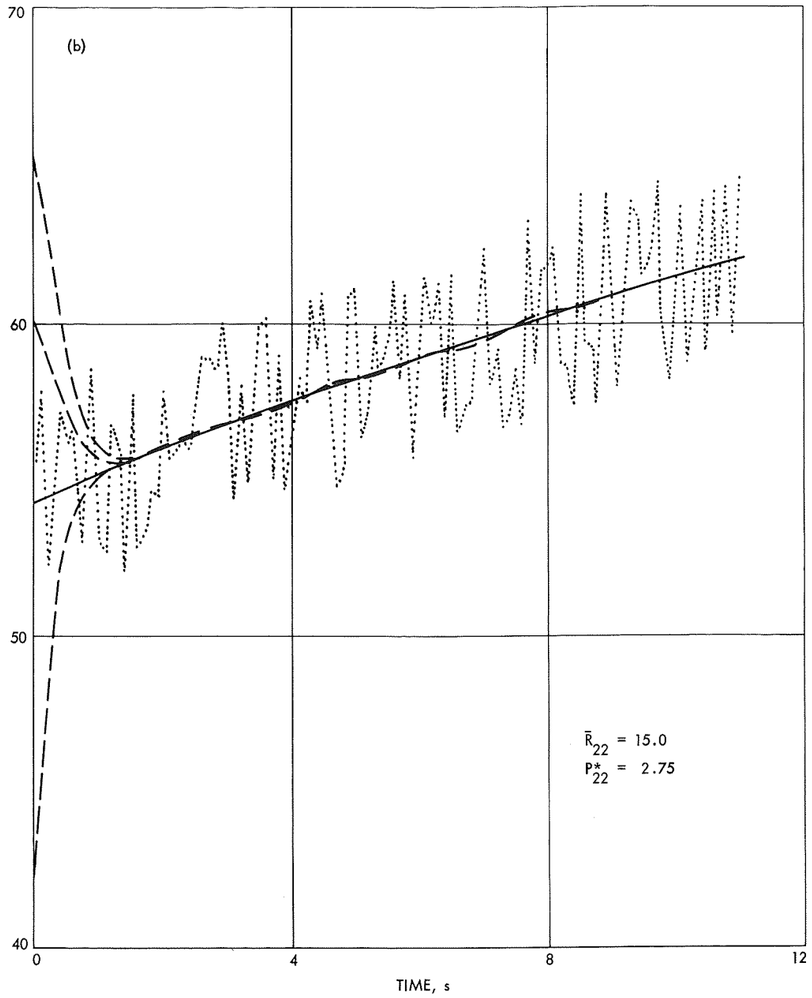

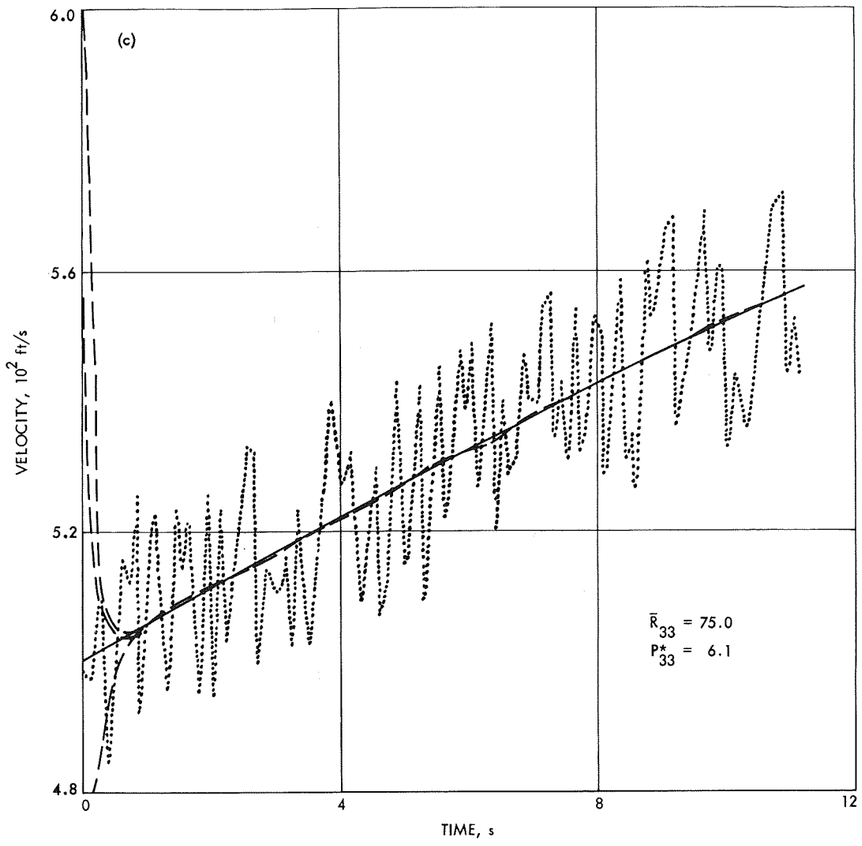

Fig. 4. Diagonal filter with time-varying gains (linear observations)

Page intentionally left blank

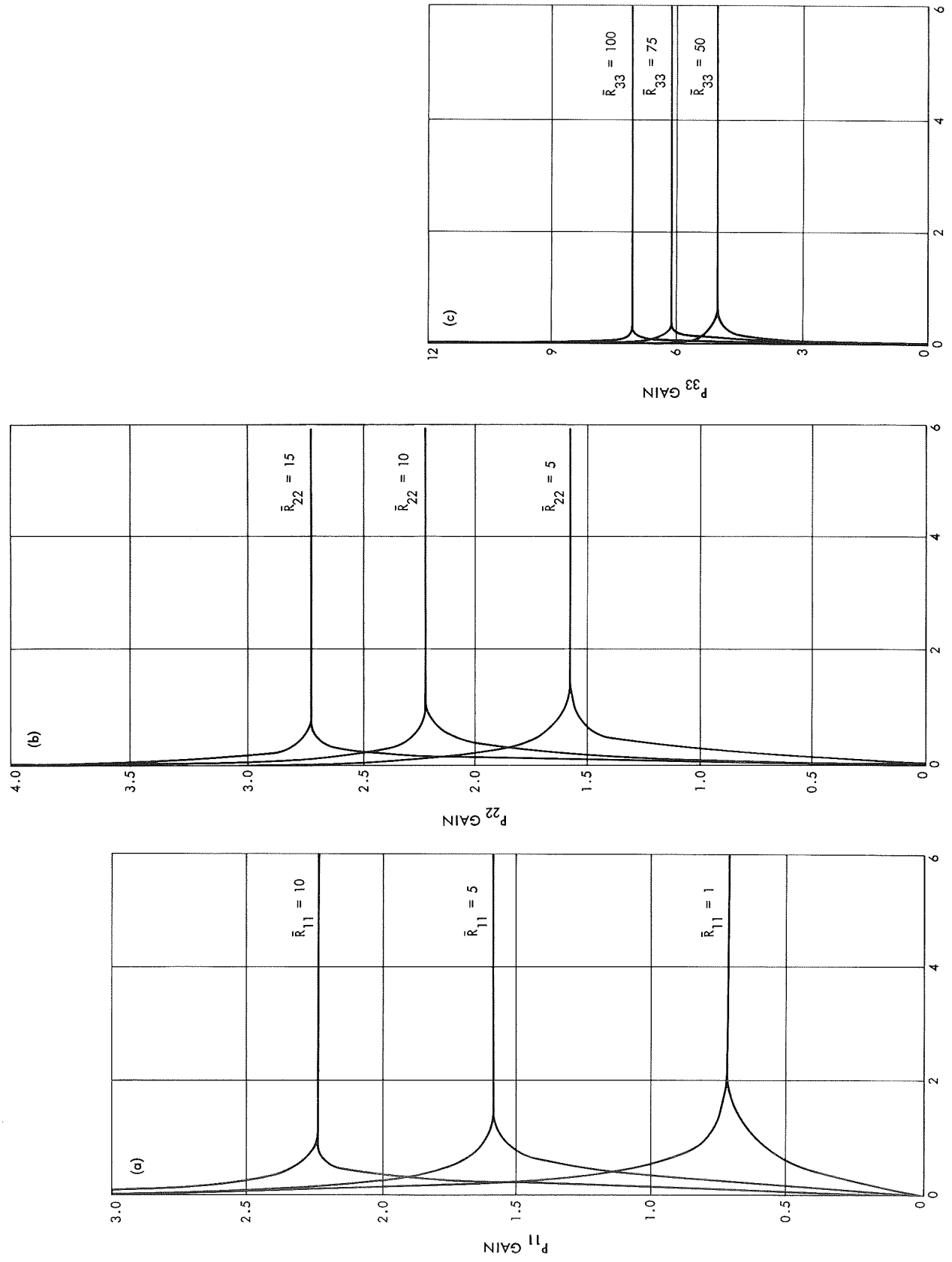

Fig. 5. Time behavior of gains in a diagonal filter (linear observations)

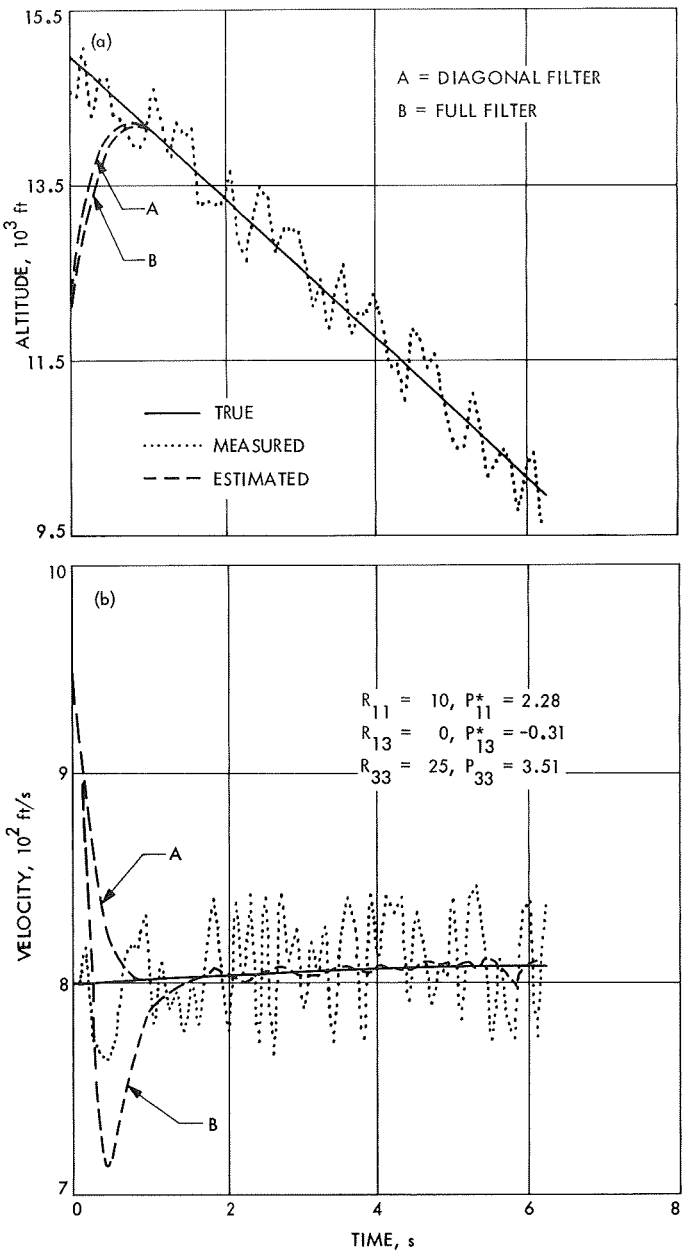

Fig. 6. Full and diagonal filters with time-varying gains (linear observations)

The curves of Fig. 7 display the behavior of the gain equations of the full filter as a function of the applied R_{13} values and applied initial conditions on P_{ij}, keeping the values of R_{11} and R_{33} fixed. The results can be summarized as follows:

(1) The gain equations P_{ij} settle to the same constant values for a given set of R_{ij} values despite the change of the initial conditions on the gain differential equations. The settled values of P_{ij} are dependent only on the selected set of R_{ij} values.

(2) For given values of R_{11} and R_{33} there exists a value for R_{13} for which $\dot{P}_{13} = P_{13} \equiv 0$ after a short transient time. This is clearly shown in the set of curves in Fig. 7, where the condition $\dot{P}_{13} = P_{13} \equiv 0$ is obtained by $R_{13} = 3.5$ after 0.6 s. It is noted that, for changing the values of R_{11} and R_{33}, there exists another corresponding value of R_{13} for which $\dot{P}_{13} = P_{13} \equiv 0$ after a short transient time.

(3) For a given set of R_{11} and R_{33} values, the change in R_{13} results only in small changes in the settled values of P_{11} and P_{33}, as shown in Fig. 7. This means that there is only a very weak coupling between the diagonal and off-diagonal gain differential equations.

The result summarized under item (2) above is the most interesting and important. That result forms the mathematical explanation and justification for the diagonally reduced simplified filter which is described by proposition 1. In view of the result noted in item (2), the disregarding of all but the diagonal gain equations in the filtering scheme is, in effect, equivalent to choosing the R_{ij} values such that $\dot{P}_{ij} = P_{ij} \equiv 0$ after a short transient time.

The condition $\dot{P}_{ij} = P_{ij} \equiv 0$ in (t_1,t_2) is, in effect, a diagonally reduced filter almost in the entire time interval $(0,t_2)$, since $\Delta t = t_1 \ll t_2$. The dynamics of the diagonal filter (where $P_{ij} = \dot{P}_{ij} \equiv 0$ from $t = 0$) and the dynamics of the full filter (with R_{ij} values yielding $\dot{P}_{ij} = P_{ij} \equiv 0$ after Δt transient time) are different only during the transient part of the filtering process, when $\dot{P}_{ij}$ and P_{ij} in the full filter scheme are still different from zero. It has to be noted, however, that the diagonal filter effects shorter and smoother transient estimates than the corresponding full filter even if it is operated with such R_{ij} values which yield $\dot{P}_{ij} = P_{ij} \equiv 0$ after a Δt transient time.

It is interesting to note that the full filter, even if it is operated with proper R_{ij} values which yield $\dot{P}_{ij} = P_{ij} \equiv 0$ after a short transient time, has a tendency to allow sections to diverge on the transient parts of the estimated trajectories. Thus, it can be concluded that the off-diagonal gain equations do not contribute to the filter's tracking performance in a positive sense in the investigated class of cases. They represent redundant operations in the filtering process and degenerate the filter's tracking performance.

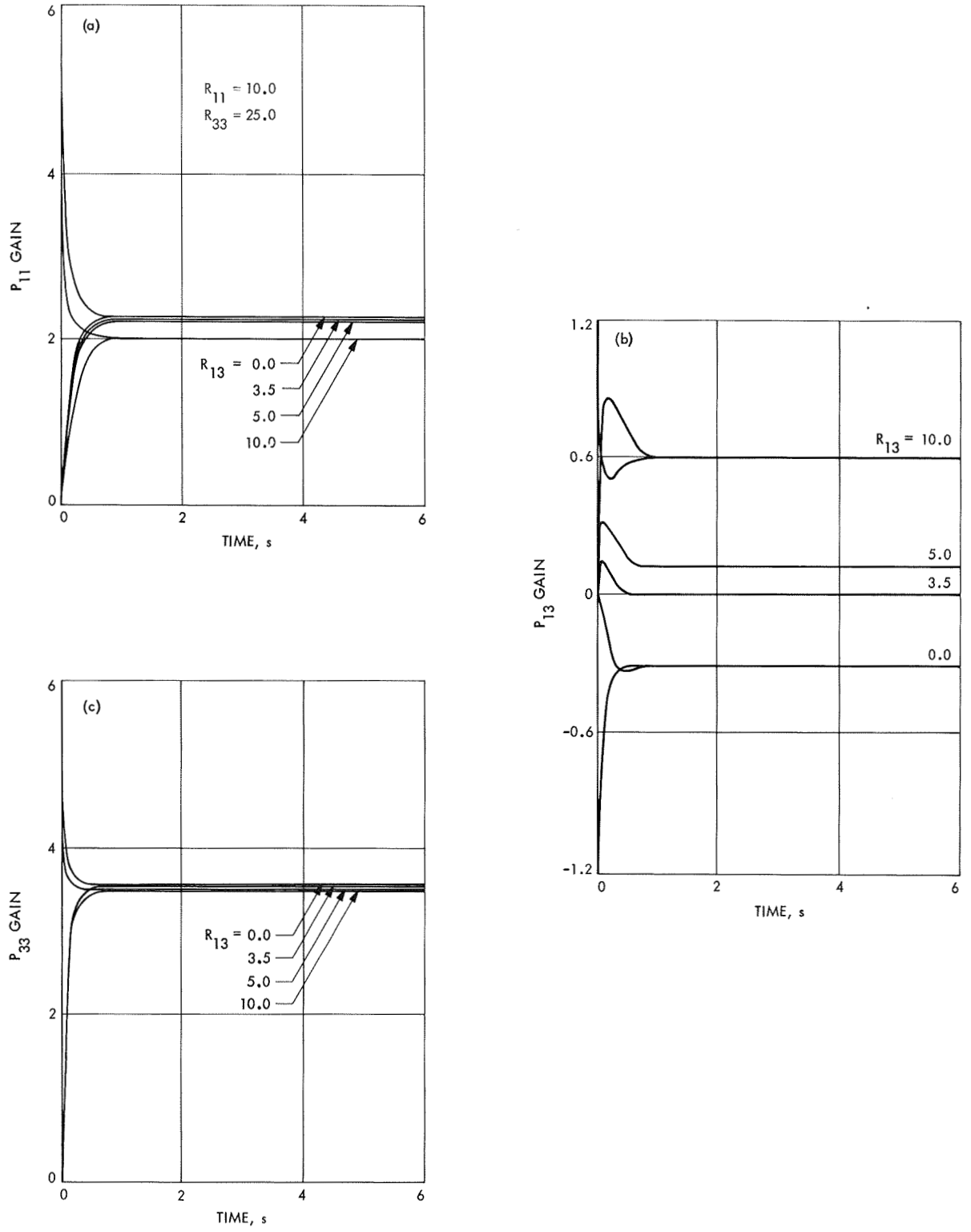

Fig. 7. Time behavior of gains in a full filter (linear observations; vertical descent)

Alternatively, it can also be stated that the diagonal filter in the investigated cases yields converging estimates at least as good as the full filter. If this is true generally, there is certainly no need for implementing the full filter scheme.

B. Nonlinear Observations

When proposition 1 is applied to Eqs. (C-4) through (C-12) in Appendix C, the time-varying diagonally reduced filter for sequentially estimating altitude, path angle, and velocity—given noisy nonlinear observations on all states—is composed of the following set of ordinary nonlinear differential equations:

$$\dot{\hat{x}}_1 = -\hat{x}_3 \sin \hat{x}_2 + \frac{2}{c} P_{11} \left(y_1 - \frac{\hat{x}_1}{c} \right) \tag{24}$$

$$\dot{\hat{x}}_2 = \left(\frac{g}{\hat{x}_3} + \frac{\hat{x}_3}{r} \right) \cos \hat{x}_2 + 2P_{22} \hat{x}_3 \left[y_2 \cos (\hat{x}_2 - \theta) - y_3 \sin (\hat{x}_2 - \theta) \right] \tag{25}$$

$$\dot{\hat{x}}_3 = g \sin \hat{x}_2 - K \hat{x}_3^2 \exp (-b \hat{x}_1) + 2P_{33} \left[y_2 \sin (\hat{x}_2 - \theta) + y_3 \cos (\hat{x}_2 - \theta) - \hat{x}_3 \right] \tag{26}$$

$$\dot{P}_{11} = -\frac{2}{c^2} P_{11}^2 + \overline{R}_{11} \tag{27}$$

$$\dot{P}_{22} = -2P_{22} \left(\frac{g}{\hat{x}_3} - \frac{\hat{x}_3}{r} \right) \sin \hat{x}_2 - 2P_{22}^2 \hat{x}_3 \left[y_2 \sin (\hat{x}_2 - \theta) + y_3 \cos (\hat{x}_2 - \theta) \right] + \overline{R}_{22} \tag{28}$$

$$\dot{P}_{33} = -4P_{33} K \hat{x}_3 \exp (-b \hat{x}_1) - 2P_{33}^2 + \overline{R}_{33} \tag{29}$$

Again, the time-varying diagonally reduced filter scheme, given by Eqs. (24–29), has a much simpler structure than the full filter scheme given by Eqs. (C-4) through (C-12) in Appendix C. The new features of the time-varying diagonal filter scheme with nonlinear observations as compared to the corresponding full filter scheme are the following:

(1) The dimensionality of the filter scheme is reduced from 9 to 6.

(2) The terms in the diagonal gain equations are reduced by a factor of 4.

(3) The diagonal gain equations are decoupled from each other.

(4) There is only one gain term in Eqs. (24–26) which takes care of the running observations.

(5) The state-dependent coefficients of the linear terms in Eqs. (27–29) are the second and third diagonal elements of the Jacobian of the system equations [given by Eq. (B-3), Appendix B], while the state-dependent coefficients of the quadratic terms in those equations are the diagonal elements of the Jacobian [given by Eq. (C-3), Appendix C] which is the second derivative of the observation vector.

(6) The meaning of the diagonal elements of the weighting matrix R is again reinterpreted in the diagonally reduced filter scheme. This is again signified by a bar over the term $\overline{R}_{ii}$.

(7) The observations explicitly appear as forcing terms in one of the gain differential equations, Eq. (28). The other two gain differential equations, Eqs. (27) and (29), are decoupled from the observations; thus, they are essentially identical to the gain differential equations, Eqs. (11) and (13), for the linear observation vector. Hence the gain differential equations of the diagonally reduced filters for the specified linear observation vector and for the specified nonlinear observation vector differ only in one gain equation. That gain equation is related to the path angle.

(8) The gain terms in the state estimator equations of the filter scheme for the nonlinear observation vector are not simply the products of the gains and the error between the estimated and measured states, as is the case when dealing with the linear observation vector. For the nonlinear observation vector the gain terms in the state estimator equations also involve state-dependent coefficients which are the first derivatives of the observation vector.

1. Input data. In the digital simulation of the time-varying diagonal filter scheme, given by Eqs. (24) through (29), the following weighting factors were applied [(A), (B), and (C) denote the curves in Fig. 8]:

(A) $\overline{R}_{11} = 20$, $\overline{R}_{22} = 10^{-4}$, $\overline{R}_{33} = 50$

(B) $\overline{R}_{11} = 10$, $\overline{R}_{22} = 5 \times 10^{-5}$, $\overline{R}_{33} = 25$

(C) $\overline{R}_{11} = 2$, $\overline{R}_{22} = 10^{-5}$, $\overline{R}_{33} = 10$

The other input data (initial conditions, noise, parameters) as well as the employed integration routine were identical to those applied for simulating the diagonal filter for a linear observation vector. (See Subsection A.)

2. General results. The main results of the digital simulations of the time-varying diagonal filter for the specified nonlinear observations are the same as those for the specified linear observations summarized in Subsection A. Hence, the essential result is the conformity of the results obtained for the specified *nonlinear* observations to those obtained for the specified *linear* observations. The conformity of the results for the two observation vectors is interesting since the gain differential equations differ somewhat in the two filter schemes.

A typical set of results is presented in Fig. 8. These curves clearly demonstrate that the tracking performance and stability of the diagonal filter are satisfactory. The simplified filter tracks the true trajectories sufficiently smoothly after a short (1.0 s) transient time. Further, the response of the simplified filter to the wrong initial estimates on the state variables is also excellent. The curves also illustrate how the changes in the values of the weighting factors $\overline{R}_{ii}$ affect the filter's tracking performance. The high $\overline{R}_{ii}$ values yield shorter transient parts than the low $\overline{R}_{ii}$ values, while the low $\overline{R}_{ii}$ values yield slightly smoother estimated trajectories.

The curve sets shown in Fig. 9 show how the time behavior of the gain equations of the diagonal filter depend on the applied weighting factors $\overline{R}_{ii}$ and on the applied initial conditions of P_{ii}. The gain equations of the diagonal filter scheme settle to some constant values after a short transient time in each case. The settled values of P_{ii} depend strongly on the selected values of $\overline{R}_{ii}$ but are not dependent on the applied initial conditions. This result is of great importance with regard to the response characteristics and stability of the diagonal filter.

The fact that the different P_{ii} gains, for identical values of $\overline{R}_{ii}$, settle to almost the same constant values can again be explained by the relative insignificance of the linear terms in the gain equations of the diagonal filter. In this connection, it is interesting to note that the differential equation for the P_{22} gain also settles to constant values despite the strongly state- and observation-dependent coefficient of the quadratic term in Eq. (28). It should be emphasized, however, that the weighting factors and the settled steady-state values belonging to the differential equation for the P_{22} gain (for the nonlinear observation vector) are five or six orders of magnitude smaller than the weighting factors and settled values which belong to the differential equation for the P_{22} gain (linear observation vector). (Compare curves of Fig. 9 with the P_{22} curves shown in Fig. 5.)

The reliability of the diagonal filter was again tested by applying it to sequentially estimating the state vector in different regions of the state space. In doing so, the filter's good response characteristics and stability remained unchanged.

V. Constant-Gain Diagonal Filter

In the preceding section it was emphasized that the gain differential equations of the diagonal filter settle to constant values after a short transient time in each of the investigated cases. This specific behavior of the gains was exhibited even by the simulated full filter. Furthermore, it has to be noted that the transient parts of the estimated trajectories and the transient parts of the corresponding gains did exhibit a one-to-one correspondence on the time scale. Hence, the general result may concisely be stated as follows: the diagonal filter scheme yields a constant algebraic structure for the gains; the diagonal filter tracks the true trajectories from that point on where the gains settle to constant values; the constant gains provide stable and sufficiently smooth estimated trajectories.

The very existence of the settled values of the gains and the associated stable and smooth tracking performance of the diagonal filter suggests the idea set forth by proposition 2 (Section III-A). Following that proposition, the settled values of the diagonal filter will now be applied as constant gains in the diagonally reduced filter scheme from the initiation of sequential estimation for the specified linear and nonlinear observation vectors. Thus, the on-line solution (or mechanization) of all gain equations will be omitted in the filtering process.

A. Linear Observations

According to proposition 2, the constant-gain diagonal filter for sequentially estimating altitude, path angle, and velocity, given noisy linear observations on all states, becomes [from Eqs. (8–10)]:

$$\dot{\hat{x}}_1 = -\hat{x}_3 \sin \hat{x}_2 + 2P^*_{11}(y_1 - \hat{x}_1) \tag{30}$$

$$\dot{\hat{x}}_2 = \left(\frac{g}{\hat{x}_3} - \frac{\hat{x}_3}{r}\right) \cos \hat{x}_2 + 2P^*_{22}(y_2 - \hat{x}_2) \tag{31}$$

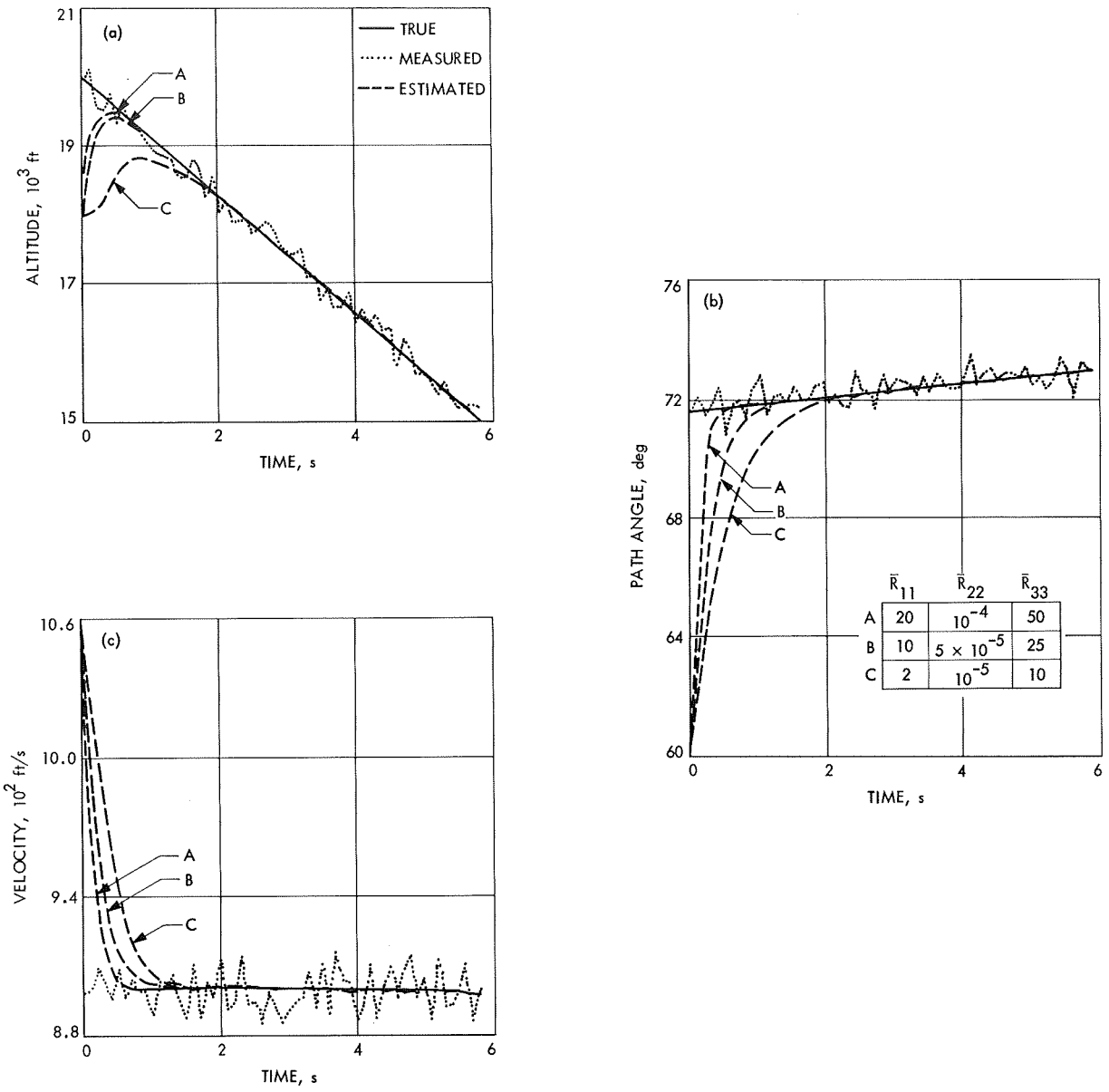

Fig. 8. Diagonal filter with time-varying gains (nonlinear observations)

$$\dot{\hat{x}}_3 = g \sin \hat{x}_2 - K\hat{x}_3^2 \exp(-b\hat{x}_1) + 2P_{33}^*(y_3 - \hat{x}_3) \tag{32}$$

where now P_{ii}^* are constants, the settled values of the P_{ii} equations in the corresponding time-varying diagonal filter. The dynamic structure of the filter is shown with its functional components in Fig. 10.

1. Input data and results. The constant-gain diagonal filter, given by Eqs. (30–32), was simulated for the same conditions as the time-varying diagonal filter, described in Section IV-A. The filter was simulated with the following constant, settled diagonal gains:

(A) $P_{11}^* = 1.57$, $P_{22}^* = 1.57$, $P_{33}^* = 1.15$

(B) $P_{11}^* = 2.24$, $P_{22}^* = 2.73$, $P_{33}^* = 6.10$

The obtained results are depicted in Fig. 11 [(A) and (B) denote the curves]. As the curves show, the tracking performance of the constant-gain diagonal filter is very

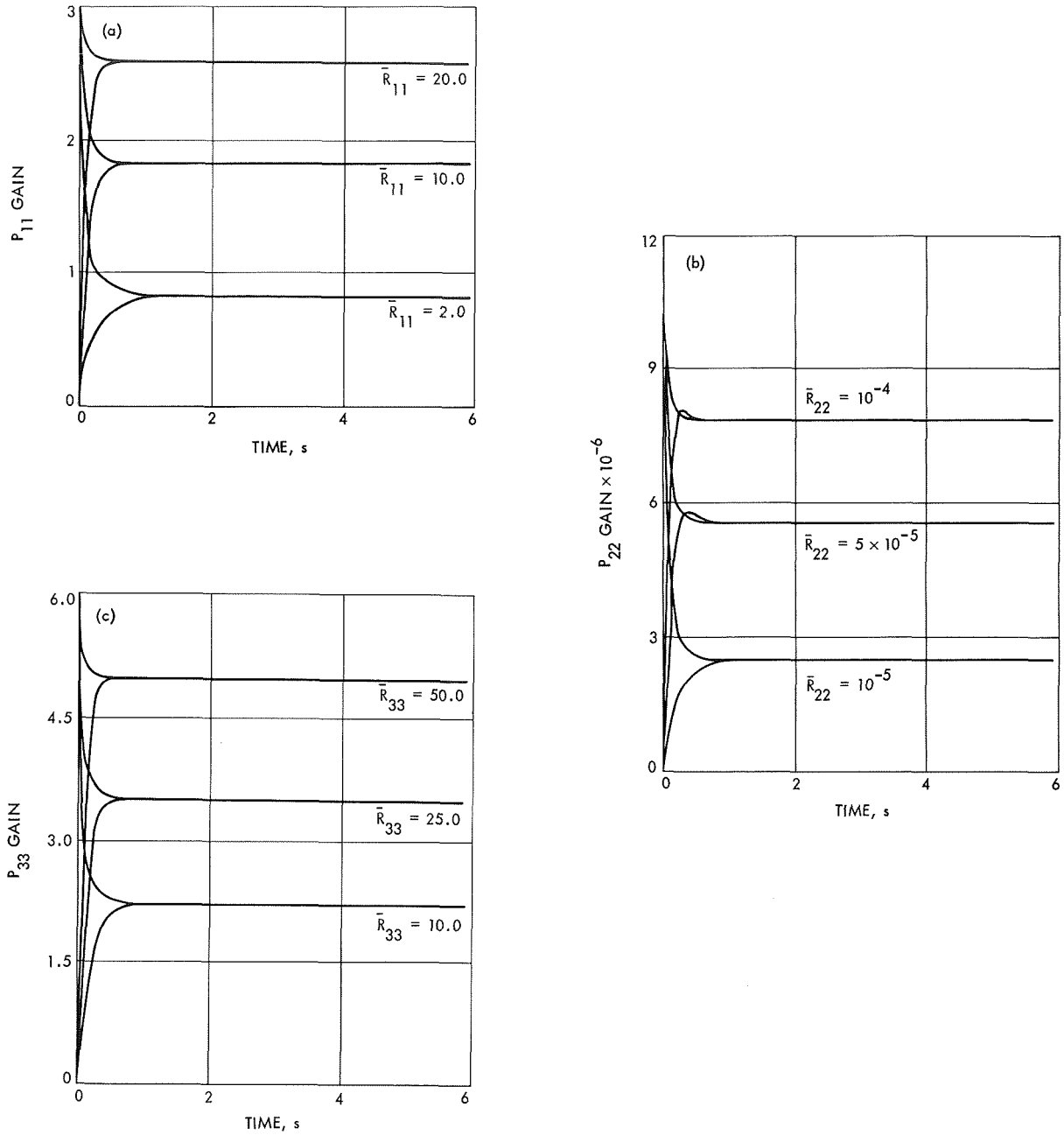

Fig. 9. Time behavior of gains in a diagonal filter (nonlinear observations)

satisfactory. What is more, it tracks slightly faster than the corresponding time-varying diagonal filter. The typical transient time is 1.0 s. The tracking characteristics of the constant-gain diagonal filter as a function of the applied constant gains completely correspond to the tracking characteristics of the time-varying diagonal filter as a function of the applied weighting factors. Thus, high constant gains yield shorter transient estimates than the low constant gains, while the low constant gains yield smoother estimates than the high constant gains. The response of the constant-gain diagonal filter to the wrong initial estimates on the states is also very stable.

2. Comparison of the constant-gain diagonal and full filters. When simulating the MPLS nonlinear filter for a vertical trajectory problem it was found in Section IV-A that the gain equations of the full filter also settle to constant values after a short transient time. To illustrate

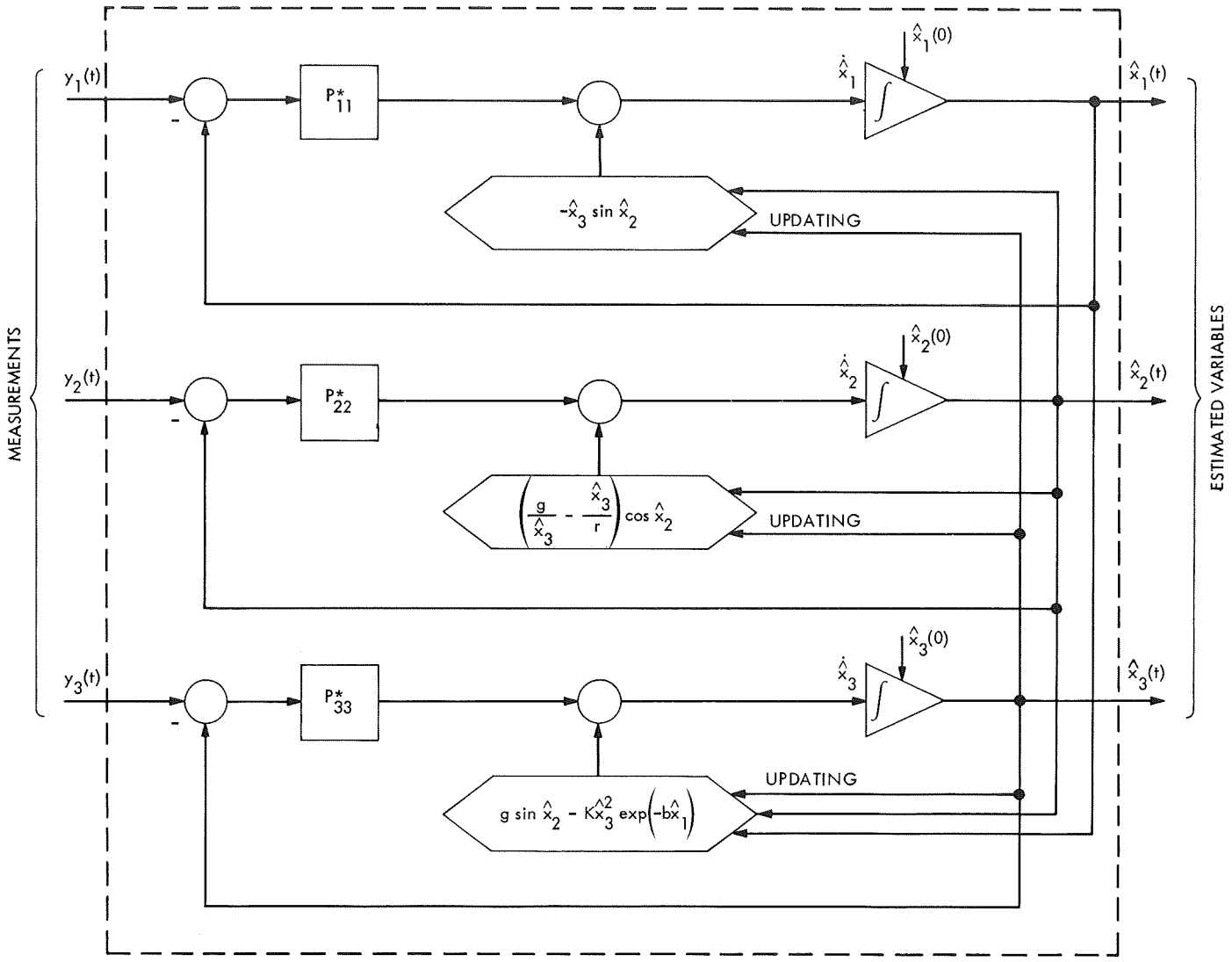

Fig. 10. Functional configuration of a constant-gain diagonal filter (linear observations)

the significance of the diagonal structure of the constant-gain filter scheme regarding the filter's tracking performance, it is now compared to the tracking performance of the full filter scheme where also constant gains are applied from the initiation of the sequential estimation.

The constant-gain full filter equations for a vertical trajectory problem, given noisy linear observations on all states, become [from Eqs. (15) and (16)]:

$$\dot{\hat{x}}_1 = -\hat{x}_3 + 2P^*_{11}(y_1 - \hat{x}_1) + 2P^*_{13}(y_3 - \hat{x}_3) \tag{33}$$

$$\dot{\hat{x}}_3 = g - K\hat{x}_3^2 \exp(-b\hat{x}_1) + 2P^*_{13}(y_1 - \hat{x}_1) + 2P^*_{33}(y_3 - \hat{x}_3) \tag{34}$$

The constant-gain diagonal filter equations for the same problem are the same as Eqs. (33) and (34) but with $P^*_{13} \equiv 0$.

The two filter schemes were simulated with $P^*_{11} = 2.28$, $P^*_{13} = -0.3$, $P^*_{33} = 3.51$ constant gains. The obtained results are depicted in Fig. 12. As these curves show, the tracking performance of the constant-gain diagonal filter is considerably better than the tracking performance of the constant-gain full filter., Consequently, the cross-correlated (off-diagonal) gain term degrades the filter's tracking performance in this case. It must be noted, however, that choosing $P^*_{13} \equiv 0$ for the entire filtering process also may be interpreted as the realization of a constant-gain full filter since there exists

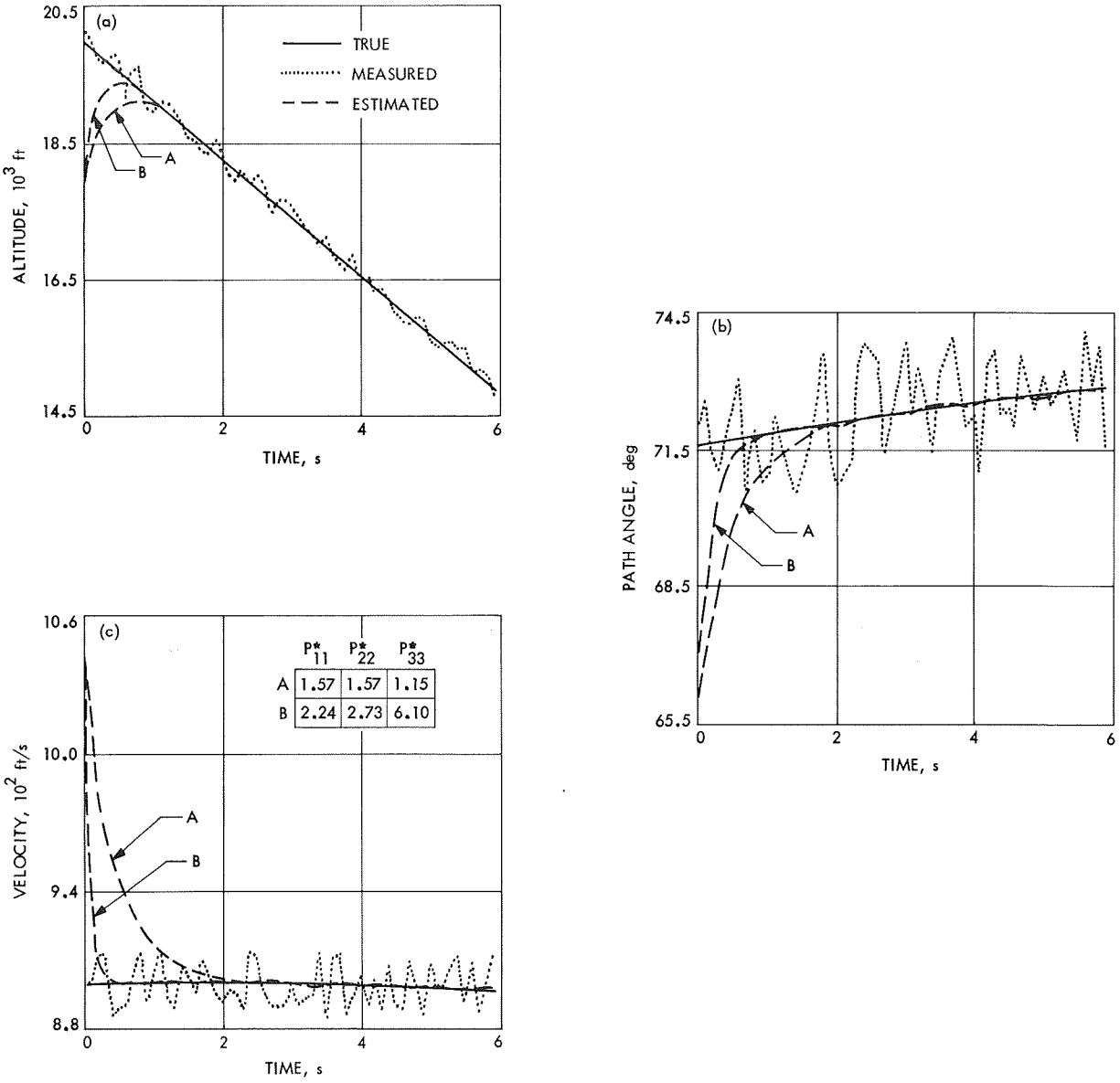

Fig. 11. Constant-gain diagonal filters (linear observations)

a weighting number R_{13} for which P_{13} stabilizes at zero after a short transient time. (See the curves in Fig. 7 and Section IV-A-3.)

B. Nonlinear Observations; Input Data and Results

According to proposition 2, the constant-gain diagonal filter for sequentially estimating altitude, path angle, and velocity, given noisy nonlinear observations on all states, becomes [from Eqs. (24–26)]:

$$\dot{\hat{x}}_1 = -\hat{x}_3 \sin \hat{x}_2 + \frac{2}{c} P^*_{11}\left(y_1 - \frac{\hat{x}_1}{c}\right) \tag{35}$$

$$\dot{\hat{x}}_2 = \left(\frac{g}{\hat{x}_3} - \frac{\hat{x}_3}{r}\right)\cos \hat{x}_2 + 2P^*_{22}\hat{x}_3\left[y_2 \cos\left(\hat{x}_2 - \theta\right) - y_3 \sin\left(\hat{x}_2 - \theta\right)\right] \tag{36}$$

$$\dot{\hat{x}}_3 = g \sin \hat{x}_2 - K\hat{x}_3^2 \exp\left(-b\hat{x}_1\right) + 2P^*_{33}\left[y_2 \sin\left(\hat{x}_2 - \theta\right) + y_3 \cos\left(\hat{x}_2 - \theta\right) - \hat{x}_3\right] \tag{37}$$

where now P^*_{ii} are constants, the settled values of the P_{ii} gain equations in the corresponding time-varying

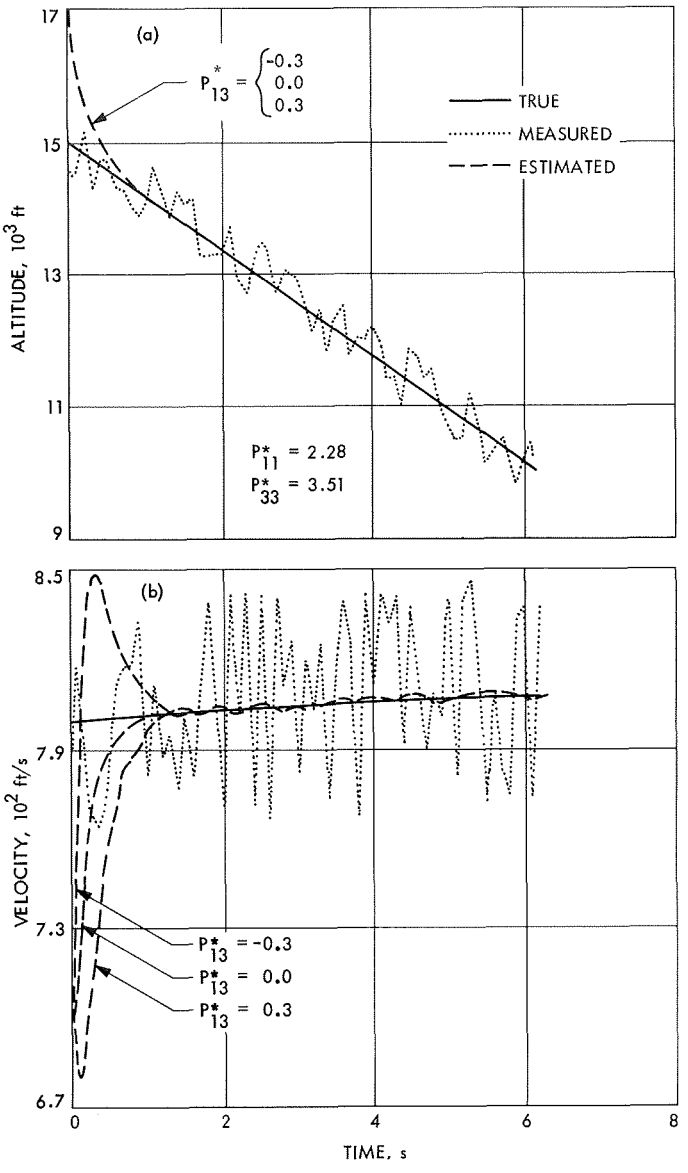

Fig. 12. Constant-gain full and diagonal filters (linear observations; vertical descent)

diagonal filter. The dynamic structure of the filter [Eqs. (35–37)] is shown in its functional configuration in Fig. 13. The constant-gain diagonal filter, given by Eqs. (35–37) was simulated with the following, constant, diagonal gains:

(A) $P^*_{11} = 2.6, \quad P^*_{22} = 7.8 \times 10^{-6}, \quad P^*_{33} = 5.0$

(B) $P^*_{11} = 1.8, \quad P^*_{22} = 5.5 \times 10^{-6}, \quad P^*_{33} = 3.5$

(C) $P^*_{11} = 0.8, \quad P^*_{22} = 2.5 \times 10^{-6}, \quad P^*_{33} = 2.2$

The obtained results are depicted in Fig. 14 [(A), (B), and (C) denote the curves]. Here again, it is seen that the tracking performance of the constant-gain diagonal filter is as good as that of the time-varying diagonal filter. The tracking characteristics of the constant-gain diagonal filter and the time-varying diagonal filter are identical. Thus, the low constant gains result in smoother estimates than the high constant gains, while the high constant gains yield faster transient estimates than the low constant gains.

It has to be noted that the constant-gain diagonal filters for the specified linear and nonlinear observation vectors differ only in the values of the P^*_{22} constant gains and in the coefficients of the corresponding gain terms. For a linear observation vector these coefficients are constants, while for a nonlinear observation vector they are state-dependent.

C. Merits of the Constant-Gain Diagonal Filter

The merits of the simplifications associated with the constant-gain diagonal filter can best be evaluated in terms of the numerical operations involved in the solution (or mechanization) of the filters. The constant-gain diagonal filter equations involve approximately only 15–25% of the numerical operations which are needed to solve the corresponding time-varying diagonal filter equations. On the other hand, the time-varying diagonal filter equations involve approximately only 10–15% of the numerical operations necessary to solve the corresponding full filter equations. Hence, the application of the constant-gain diagonal filter scheme for estimation purposes implies approximately 95–98% reduction of the numerical operations needed to solve (or mechanize) the full filter scheme. The constant-gain diagonal filter, despite its strongly simplified structure, provided considerably better tracking characteristics in the investigated cases than the time-varying diagonal filter or the full filter. The practical merits of these results are obvious.

It must be emphasized, finally, that the constant-gain diagonal filter scheme represents the ultimate simplifying reduction of the MPLS nonlinear filter.

VI. Performance of the Constant-Gain Diagonal Filter vs Partially Unknown Atmospheric Forces

In the simulation studies on the performance of the constant-gain diagonal filter, the only applied unknown

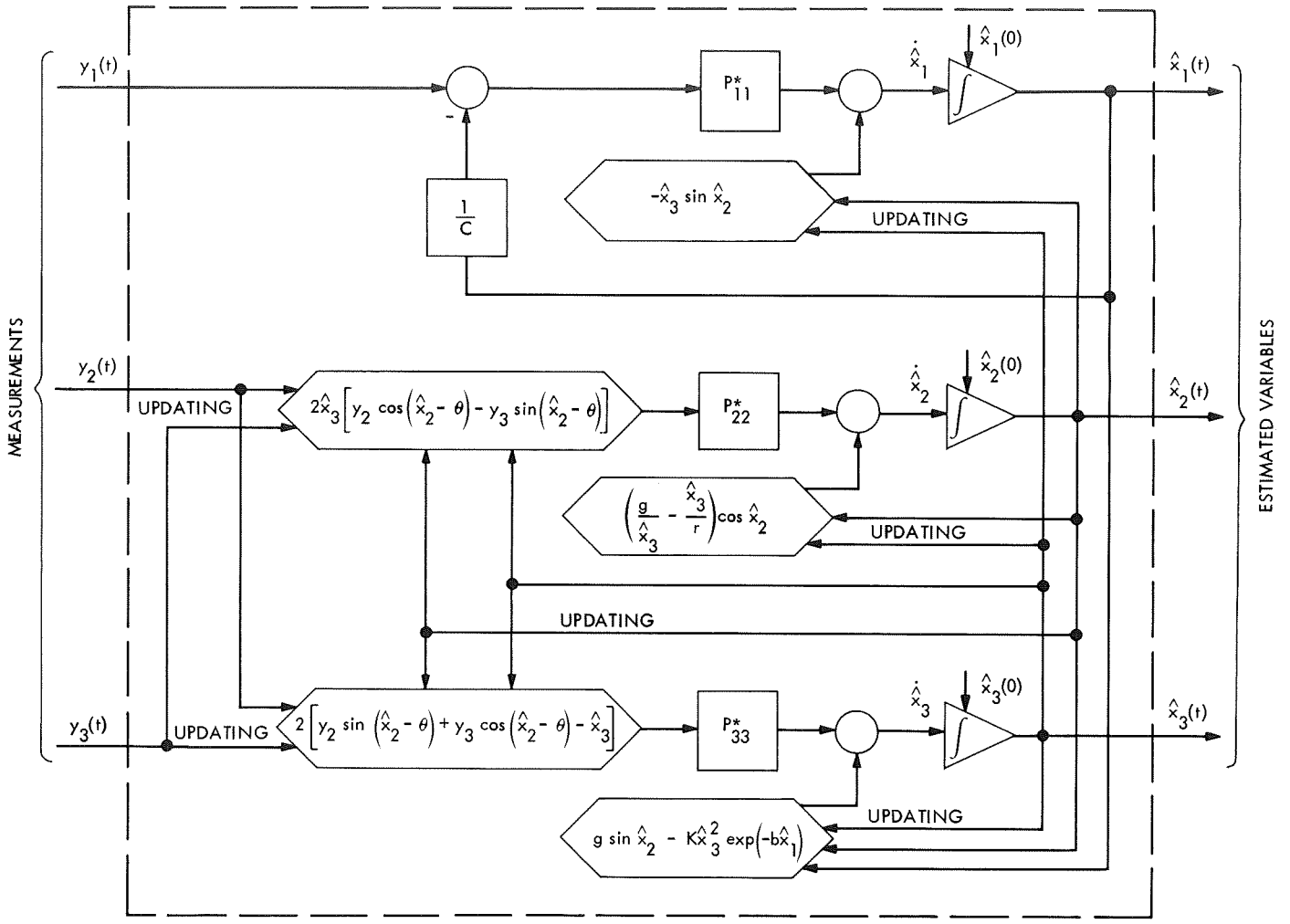

Fig. 13. Functional configuration of a constant-gain diagonal filter (nonlinear observations)

dynamic force was a uniformly distributed random dynamic disturbance added to the known deterministic forces—that is, to the gravity and drag. In other words, the same deterministic parameters were applied to simulating the *true* trajectories as well as to constructing the filter scheme. The filtering problem related to the flight of a ballistic vehicle in a partially unknown atmospheric environment, however, certainly implies acting unknown forces other than some uniformly distributed random dynamic disturbances. From the filtering point of view, a partially unknown atmospheric environment also implies acting forces of deterministic, or, of systematic character (drag and wind). The question therefore arises whether the constant-gain diagonal filter is suited to sequentially estimate the current states of a ballistic vehicle the dynamic state of which is acted on by forces of deterministic or systematic character partially unknown before the flight.

The partially unknown dynamic character (magnitude and time history) of the acting drag may be accounted for in the filtering scheme by treating the constant parameters of the drag force of a given model as new state variables having zero time derivatives. Thus, the filtering scheme could be extended to include also the sequential estimation of the constant values of the parameters of a given drag-force model. This task, however, is beyond the scope of the present study,[5] since the essential aim of this study is to develop and to test well defined simplifications of the MPLS nonlinear filter scheme for such cases when the noisy measurement vector includes *all* states. The constant parameters of a model drag force, however, cannot be measured in the same way as, say, altitude and velocity—that is, independently on the

[5]This type of parameter estimation problem will be treated in a subsequent study.

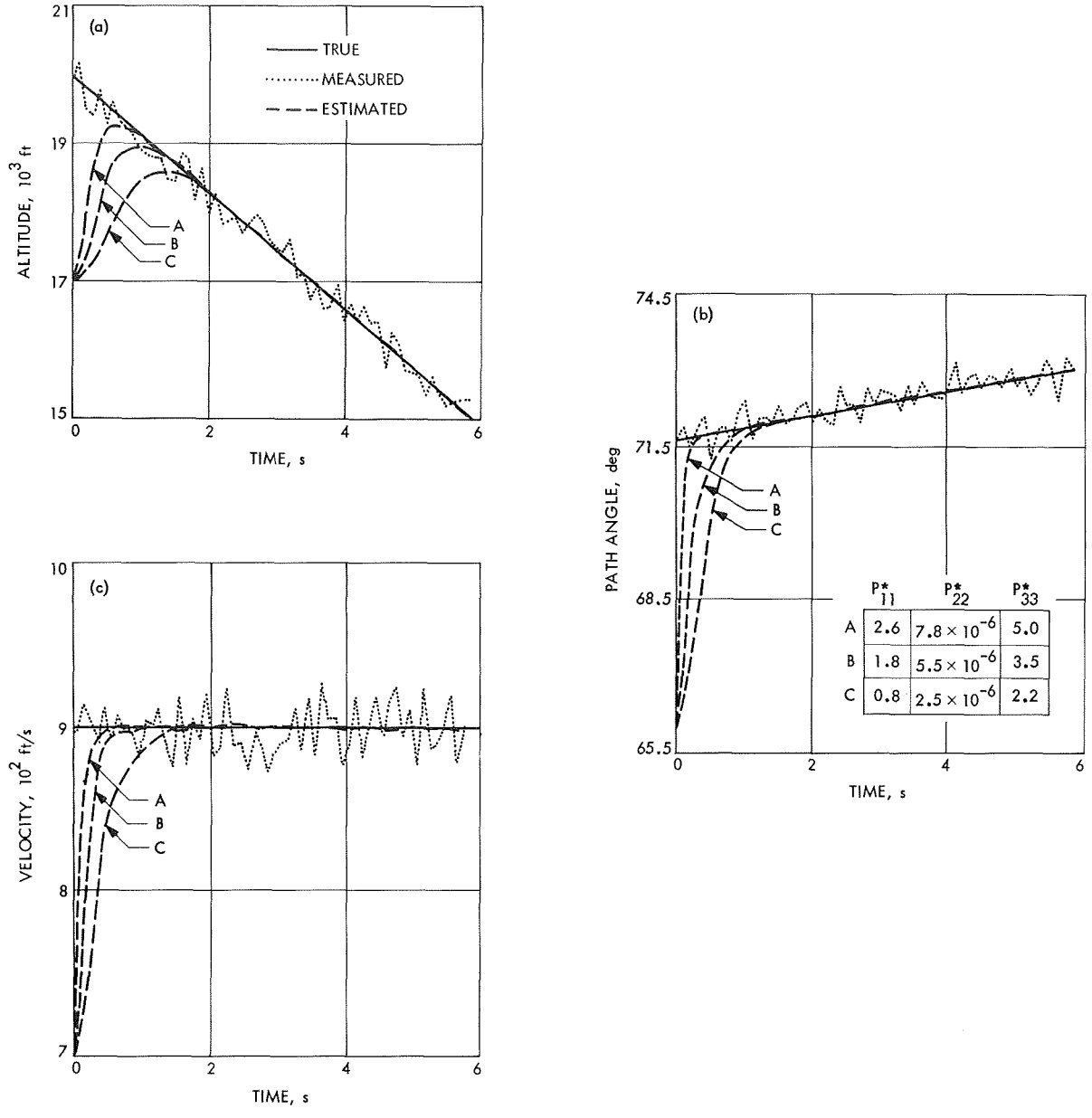

Fig. 14. Constant-gain diagonal filters (nonlinear observations)

dynamic description of the system. Now, instead of extending the filter scheme to include the estimation of parameters for producing up-to-date estimates on the dynamic states of the vehicle, the constant-gain diagonal filter will be applied in the same form as derived in Section V; that is, it will be applied in that form which is restricted to estimating only the noisy states.

A. Digital Simulation of an Unknown Situation

The application of the constant-gain diagonal filter to sequentially estimating the current states of a ballistic vehicle (whose dynamic behavior is influenced by deterministic or systematic forces partially unknown before the flight) involves the following procedure in the digital simulation of the filter.

There is a given set of constant parameters, belonging to the model drag force, which is applied in the filter equations. This set of constant parameters may be considered as the *a priori* set of parameter values.

There is another set of parameter values, belonging to the model drag force, which is applied to generate the

measurement vector by solving the system equations. This set of constant parameters may be very much (50–100%) different from that one applied in the filter equations and is considered to represent the actual situation.

In generating the measurement vector by solving the system equations, there are two forces added to the system equations which are not represented explicitly in the filter equations: wind pressure and retrothrust. The retrothrust could have been represented explicitly in the filter equations. However, to test the tracking performance of the constant-gain diagonal filter under conditions when the system's dynamic description in the filter equations is highly imprecise, some cases were simulated when the retrothrust was not represented in the filter equations.

The statistical characteristics of the random dynamic and measurement noise are being varied. In Section V a uniformly distributed random noise was applied for generating dynamic and measurement noise. Now, in addition to that, gaussian noise is introduced. This is done to test whether and how a change in the noise statistics affects the tracking performance of the constant-gain diagonal filter.

1. Input data. The atmospheric parameters applied in the filter equations correspond to the VM-7 atmosphere. These values were used throughout this study and are listed in Appendix D. The noisy measurement vector, however, was generated by applying the values of the VM-4 atmosphere. These values, for ground level density ϱ_0 and the inverse exponential scale factor b, are:

$$\varrho_0 = 4.98 \times 10^{-5} \text{ slugs/ft}^3$$
$$b = 5.89 \times 10^{-5} \text{ ft}^{-1}$$

For generating the measurement vector, a wind force and a retrothrust were applied. The wind was modeled for an asymmetrically sinusoidal time history with maximum axial intensities corresponding to 0.6–0.8 Martian gravity, according to the following expression:

$$0.5\, g\, \frac{x_3(0)}{x_3(t)} \sin\left[2\pi\, \frac{x_1(0) - x_1(t)}{x_1(\tau)}\right]$$

This model roughly corresponds to a situation when the vehicle's trajectory crosses a double-centered large-scale atmospheric turbulence.

To make the dynamic situation "more confused" for the filter, the retrothrust was switched on only in the second half of the filtering process, approximately 6.5 s after the initiation of sequential estimation. The applied retrothrust was of 1.5×10^3 lbf constant amplitude. Neither the wind nor the retrothrust was explicitly accounted for in the filter equations; they were transmitted to the filter scheme only through the actual measurements. Further, the application of the retrothrust for generating the measurement vector introduces an additional systematic error into the filter equations. This additional error is due to the depletion of the vehicle's mass which also is not represented in the filter equations.

For generating dynamic and measurement noise, the following standard deviations were applied for the gaussian disturbances. For measurements:

$$\left.\begin{aligned} \sigma_1 &= 300 \text{ ft, altitude} \\ \sigma_2 &= 15 \text{ ft/s} \\ \sigma_3 &= 30 \text{ ft/s} \end{aligned}\right\} \text{ body-referenced velocity components}$$

For dynamic noise:

$$\sigma_4 = 6 \text{ ft/s}^2, \text{ acceleration}$$

When the noise was generated by uniformly distributed random numbers the relative noise amplitudes were assumed to be the same as described in Section IV-A.

The simulation studies were carried out only for the case of the nonlinear observation vector. Hence, the constant-gain diagonal filter equations are the same as Eqs. (35–37). In those equations the following constant gains were applied: $P^*_{11} = 1.8$, $P^*_{22} = 0.8 \times 10^{-5}$, $P^*_{33} = 2.2$.

2. Results. A representative set of the obtained results is shown in Fig. 15. Representative dynamic inputs, *true* as well as assumed, are depicted in Fig. 16, while Fig. 17 displays the noisy measurements on the body-referenced velocity components.

The results shown in Fig. 15 are truly remarkable: *Despite the strong mismatch of the atmospheric parameters and despite the strong unknown dynamic inputs, the constant-gain diagonal filter exhibits excellent tracking performance!* It is also clear from the curves that the change in the noise statistics from uniform distribution to normal distribution did not alter the filter's good tracking performance in any noticeable manner.

To get a close look at the tracking performance of the constant-gain diagonal filter when strong unknown dynamic inputs are applied, the time histories of the relative estimation errors *REE* and the relative measurement errors *RME* are also computed[6]:

$$REE = \frac{\hat{x}_i(t) - x_i(t)}{x_i(t)}$$

and

$$RME = \frac{y_i(t) - x_i(t)}{x_i(t)}$$

The time histories of these relative errors are displayed in Fig. 18. (The noise pattern in these figures is gaussian.) As these figures show the *REE* are less than 10% of the *RME* after a short (0.5–1 s) transient time. Hence, the *constant-gain diagonal filter* provides a very effective filtering of the measurement noise. The overall relative estimation error is approximately 0.1%.

The velocity graph of Fig. 18 shows how the relative error of the estimated velocity behaves when the retrothrust is explicitly *not* accounted for in the filter equations. In such a case there is a 0.5% *systematic* relative error in the estimated velocities after the retrothrust is turned on. The magnitude of that systematic error, however, is surprisingly small when considering the relative magnitude of the retrothrust.

In connection with Fig. 18, it should be noted that a simple integration of the system equations in that form as they are represented in the filter would yield trajectories which are 20–80% in error relative to the true trajectories during the simulated period of sequential estimation. This fact signifies the importance and strength of the filtering scheme, the essential feature of which is the proper combination of the known system equations with the running observations for sequentially estimating the states. Thus, the constant-gain diagonal filter (as applied to the simulated "unknown situation") tracks the true trajectories very well despite the strong uncertainties in the system description, and it filters out the measurement noise very effectively.

The successful tracking performance of the constant-gain diagonal filter is evidently due to the successful choice of the weight R for the system equations relative to the weight Q for the observation equations. This successful choice of the relative weights, in turn, yields those constant gains which provide the filter's good tracking performance despite the strong unknown inputs of dynamic noise and measurement noise.

[6]In these expressions: x_i = true trajectories, y_i = measured trajectories, $\hat{x}_i$ = estimated trajectories.

B. Remarks on the Interference Between the Filter's Performance and the Computational Algorithms

In the present study, the filter's tracking performance was studied by employing the continuous formulation of the filter. One obvious way to investigate how the applied computational algorithms (integration routines) interfere with the filter's tracking performance is to change the integration step size for a fixed integration routine. In doing so it is expected that, for a given set of filter parameters, the smaller the step size the faster and smoother the filter's tracking performance.

The integration step size applied throughout in the digital simulations in this study was 10 ms. A 1-ms step size did not result in any significant improvement in the filter's tracking performance. Likewise, there was no noticeable change in the filter's tracking performance when the step size was increased to 20–30 ms. Further increase of the integration step size, however, yielded noticeable changes in the smoothness of the estimated trajectories. When the step size was increased to 0.2–0.3 s, the estimated trajectories could no longer be distinguished from the noisy measurements.

For the constant-gain diagonal filter it has been found that the negative effect of the increased integration step size on the filter's tracking performance may very well be counteracted by a proper change of the constant gains. For demonstrating this point, Fig. 15 displays two sets of results. One is obtained by applying a 10-ms step size and by using $P^*_{11} = 1.8$, $P^*_{22} = 8 \times 10^{-6}$, $P^*_{33} = 2.2$ constant gains. The other set is obtained by applying a 0.1-s step size and by taking only half of the values of the constant gains listed above. Again, as shown in Fig. 15, the results are interesting. The filter's tracking performance is essentially the same in both cases, smooth and stable, only the transient parts of the estimated trajectories differ slightly. In the case of the 0.1-s step size and taking half of the gain values, the transient time is increased by a factor of two, from 0.5–1 s to 1–2 s.

The possibility of increasing the integration step size without degenerating the final tracking performance of the constant-gain diagonal filter is of great significance with respect to the real-time mechanization of the filter.

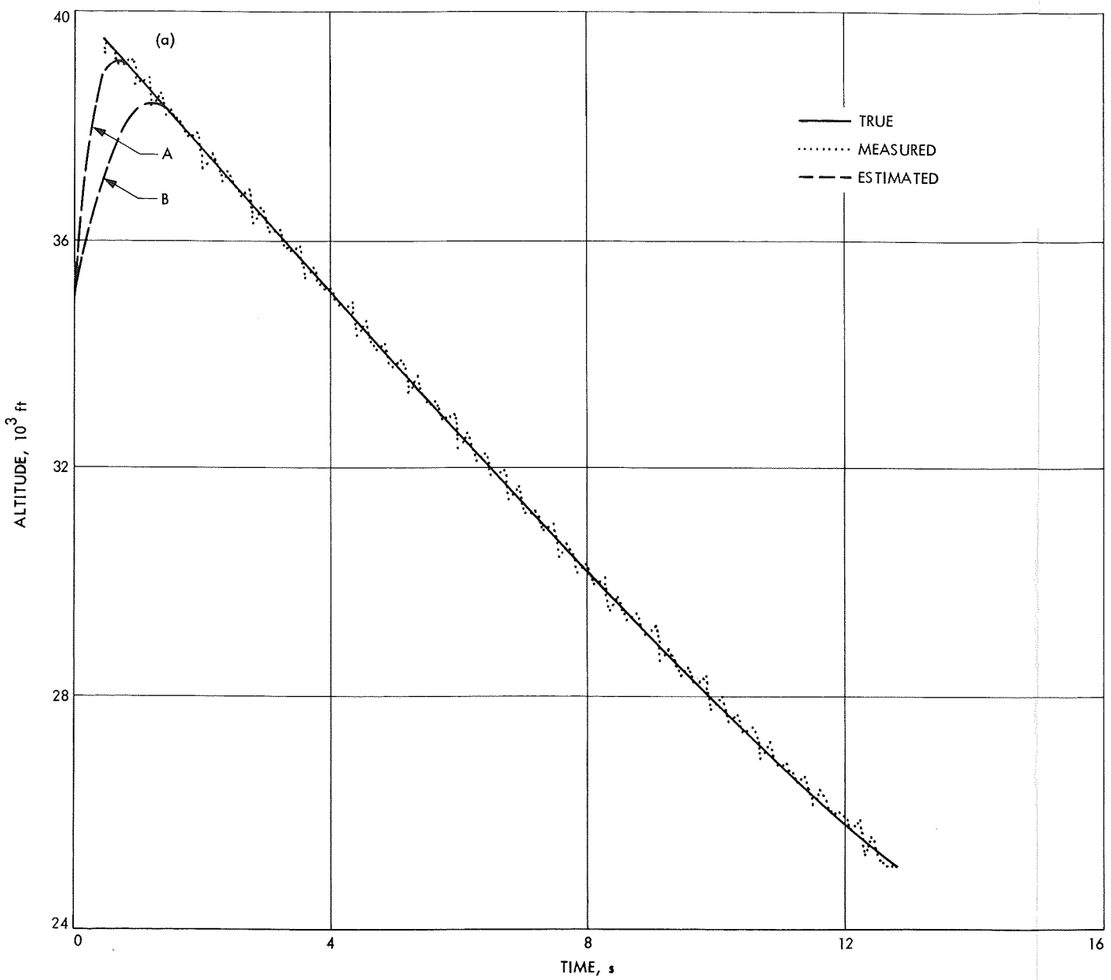
(a)
TRUE
MEASURED
ESTIMATED
A
B
ALTITUDE, 10^3 ft
40
36
32
28
24
0
4
8
12
16
TIME, s

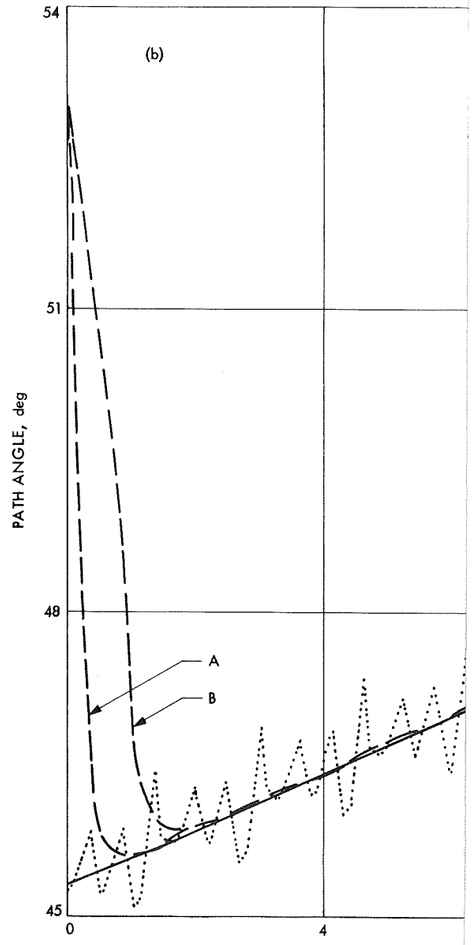
(b)
A
B
PATH ANGLE, deg
54
51
48
45
0
4

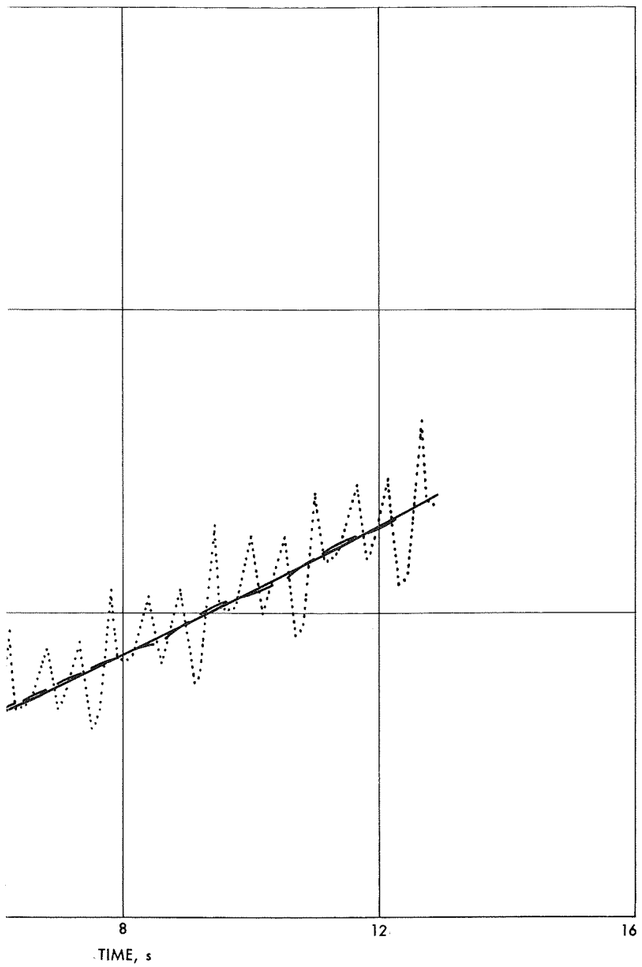

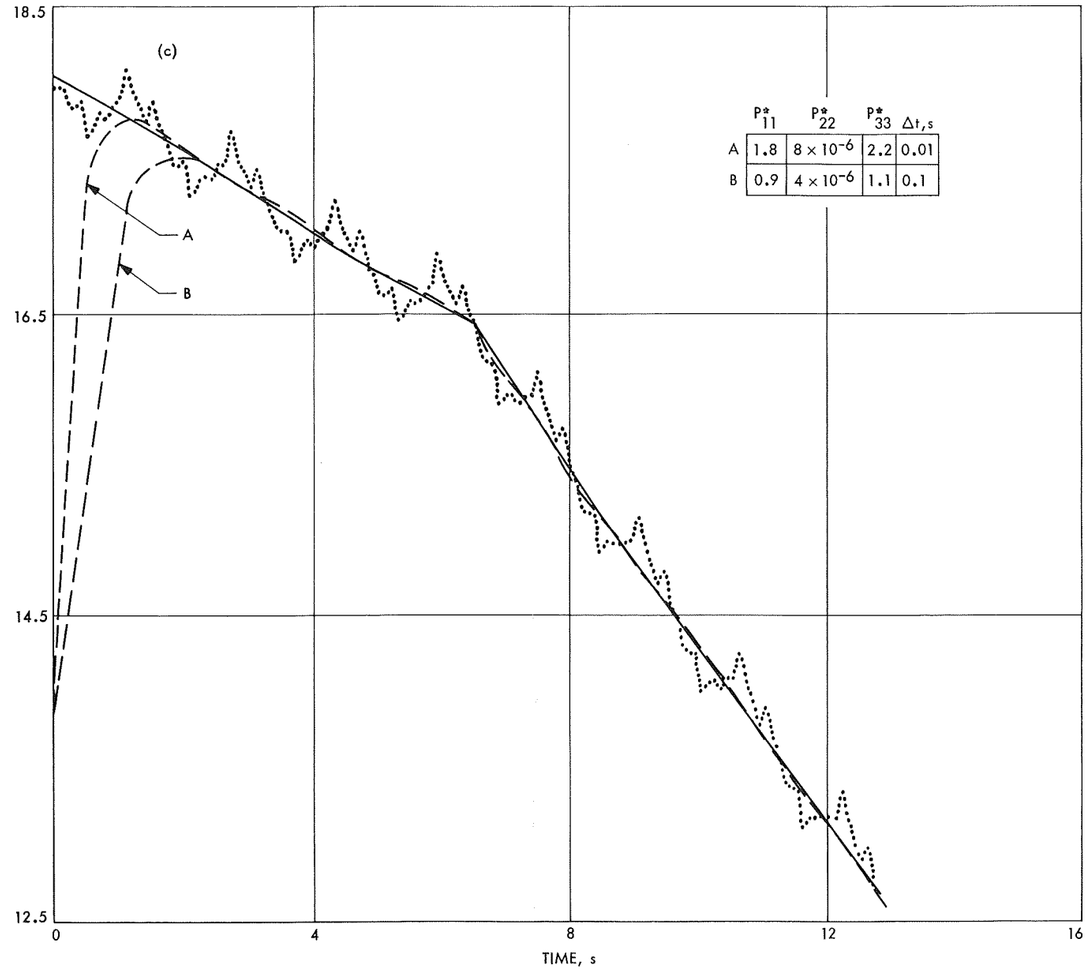

	P^*_{11}	P^*_{22}	P^*_{33}	Δt, s
A	1.8	8×10^{-6}	2.2	0.01
B	0.9	4×10^{-6}	1.1	0.1

Fig. 15. Constant-gain diagonal filters (nonlinear observations and "unknown" deterministic inputs)

Page intentionally left blank

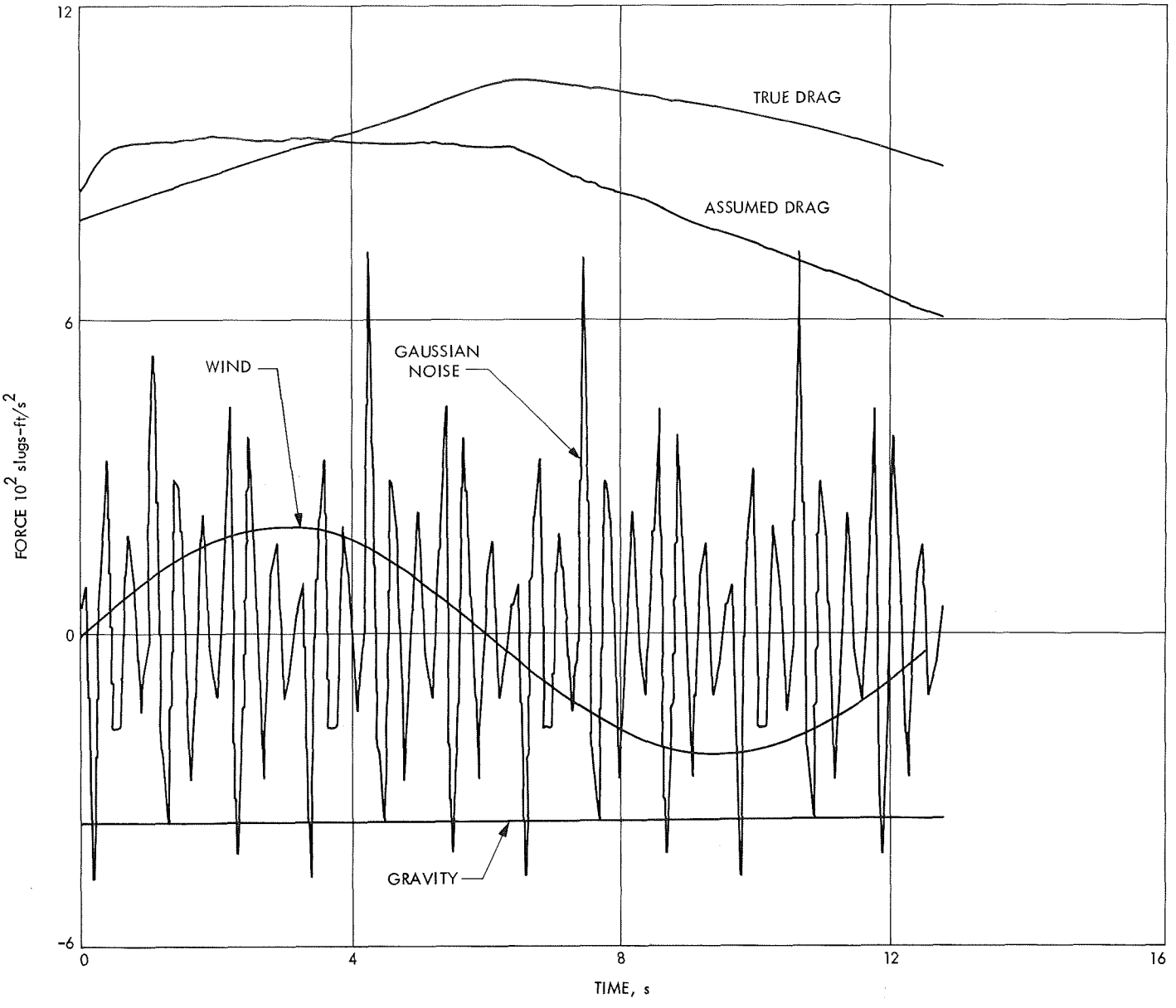

Fig. 16. True and "unknown" dynamic inputs for a constant-gain diagonal filter

VII. Summary and Conclusions

Real-time, on-line estimation of states is an essential functional part of the terminal-guidance logic having the objective of guiding a spacecraft to a soft landing on an atmosphere-bearing distant planet. Following modern concepts in the theory of estimation, nonlinear filtering by a differential-equation technique is applied to sequentially estimating the current state of a ballistic vehicle in an imperfectly known planetary atmosphere. The basic functional property of a suitably developed sequential estimator (or nonlinear filter) scheme is its feasibility for real-time implementation. Because of its deterministic derivation, the maximum principle least-squares nonlinear filter is selected for estimation purposes.

The nature of the terminal guidance problem considered in this study implies that the computations related to the digital filtering process must be executed by a special-purpose on-board computer. Consequently, the mathematical operations of filtering must not be overly complex. In this study suitable methods are developed by which the mathematical complexity of the

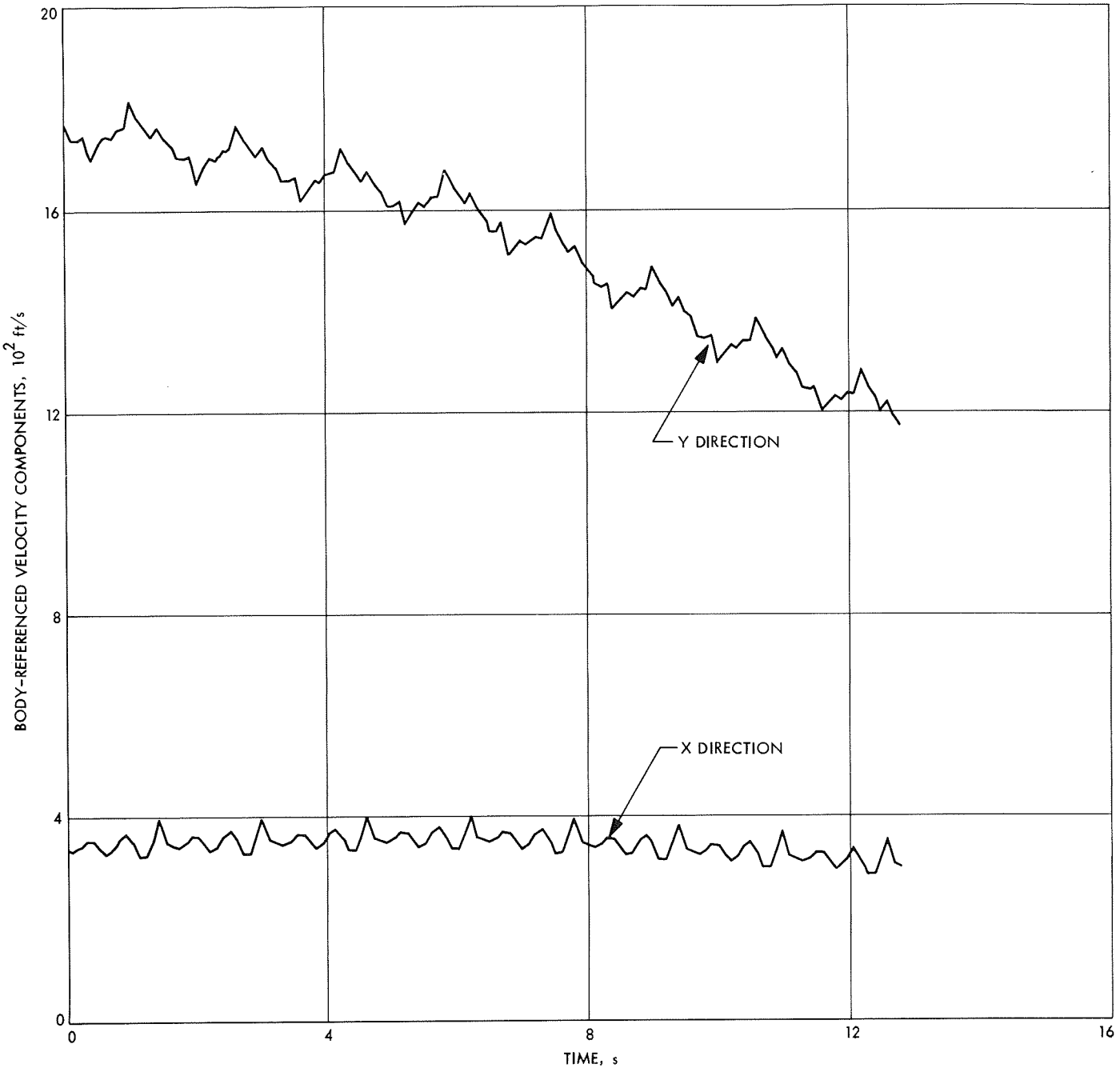

Fig. 17. Noisy measurements on body-referenced velocity components (as inputs to a constant gain diagonal filter)

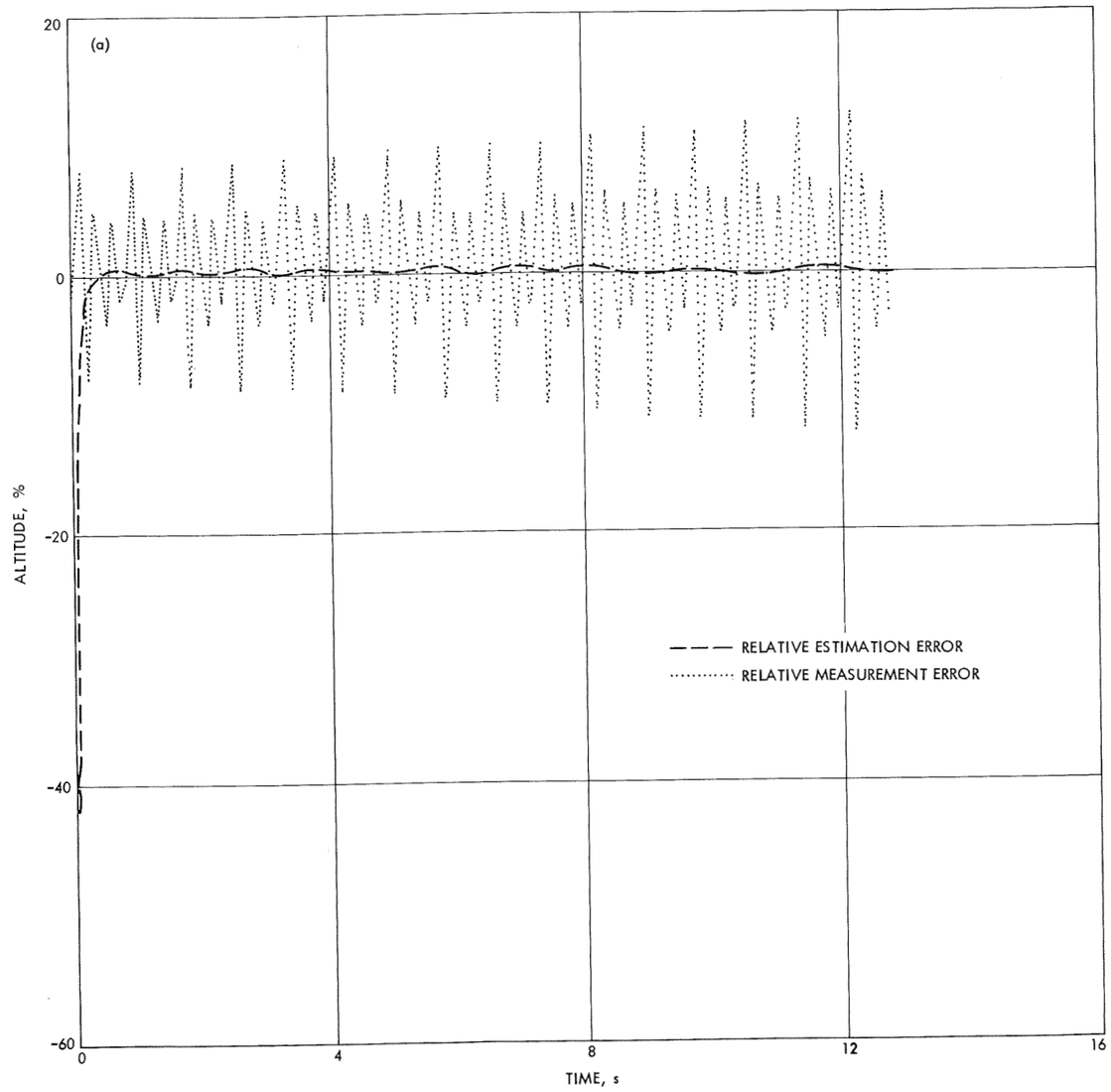
(a)
20
0
-20
-40
-60
ALTITUDE, %
0
4
8
12
16
TIME, s
RELATIVE ESTIMATION ERROR
RELATIVE MEASUREMENT ERROR

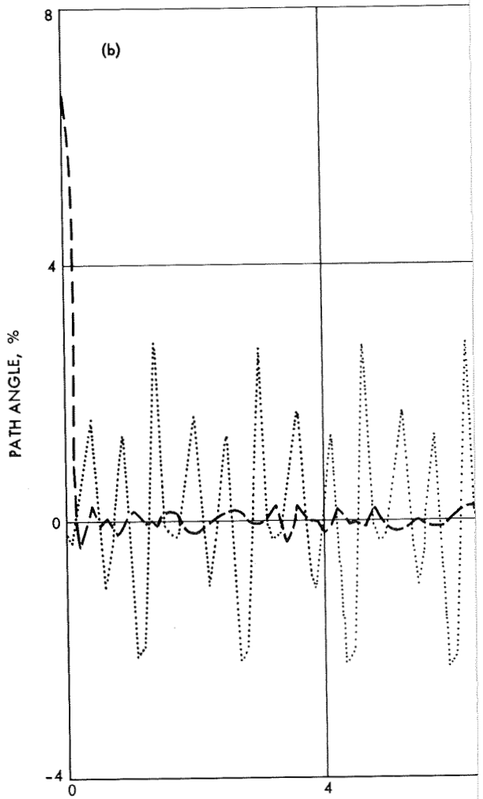
(b)
8
4
0
-4
PATH ANGLE, %
0
4

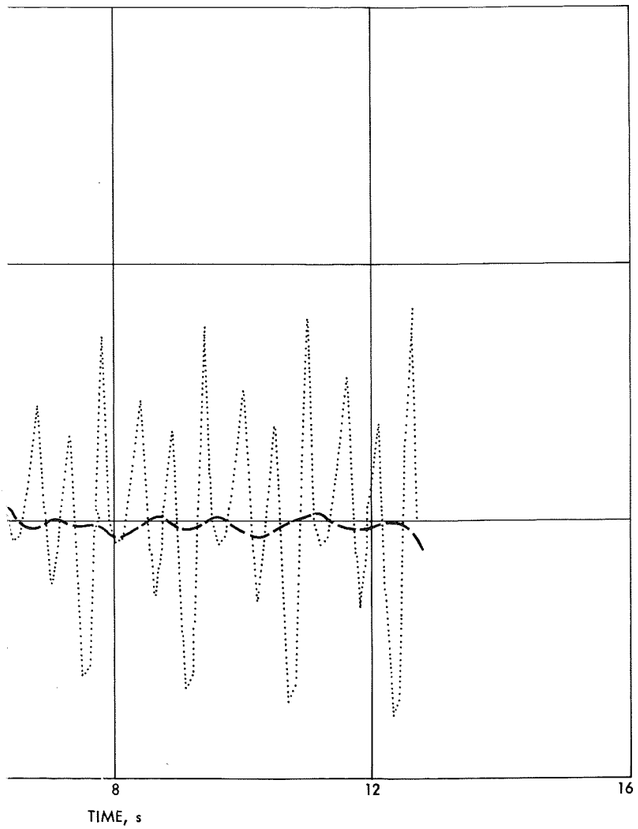

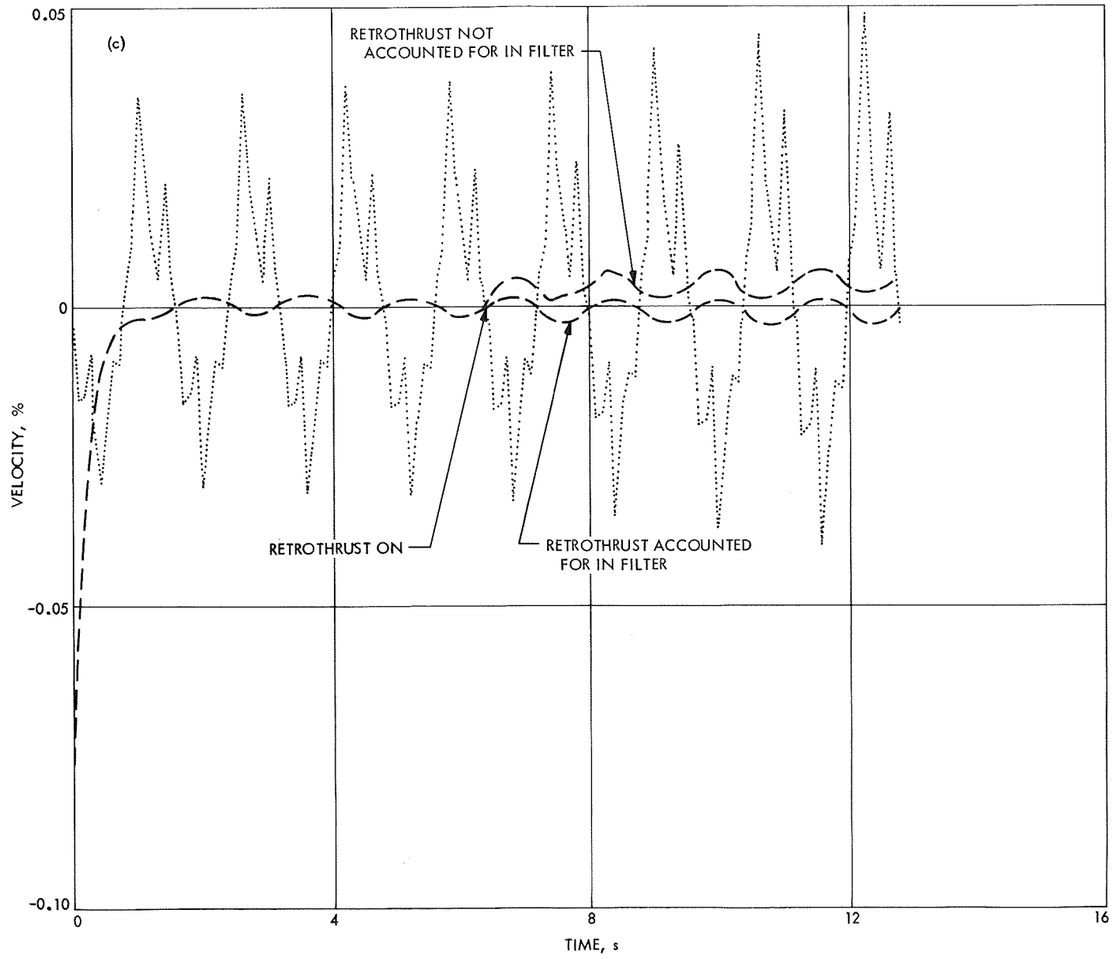

Fig. 18. Time histories of relative errors for a constant-gain diagonal filter

Page intentionally left blank

maximum principle least-squares nonlinear filter can be reduced systematically. These methods are developed for such cases when *all* states are available for linear or nonlinear measurements. The mathematical justification of the developed simplifications are briefly explained and demonstrated.

The simplifications are developed in two major steps. The first step is to reduce the dimensionality of the filter by omitting all off-diagonal gains from the filter scheme. For the resulting time-varying diagonal filter, reliable tracking performance can be assured by a judicious choice of the relative weighting factors for the residual errors. The second step is to omit even the time-varying diagonal gain equations from the filter when the diagonal gain equations stabilize to constant values after a short transient time, and to apply these settled values as constant gains from the initiation of sequential estimation.

The constant-gain diagonal filter represents the ultimate simplifying reduction of the maximum principle least-squares nonlinear filter scheme. This ultimately simplified filter scheme consists of the known system equations plus one constant-gain term which is added to each system equation. These single constant-gain terms will "transmit" all the current measurement informations on the states into the filter equations where they are solved sequentially to estimate the current value of the state vector.

The developed simplified filters are applied for sequentially estimating the states of a ballistic vehicle in an imperfectly known atmosphere. Extensive digital simulation studies were carried out to test the reliability, stability, and tracking performance of the simplified filters as applied to that particular problem. The simplified filters exhibited excellent tracking performance. Further, the simplified filters provided consistently better tracking performance than the full filters in the investigated cases. The simplified filters resulted in reliable tracking even for 100% or more mismatch of the atmospheric parameter values. This reliable tracking is due to the successful choice of the weight R for the system equations relative to the weight Q for the observation equations.

The simplified filters, applied to the ballistic state estimation problem, have the following operational characteristics:

(1) Transient time of 0.5–2.0 s.

(2) Relative errors in the estimated states are reduced to 10% or less of the relative errors in the measured states.

(3) Low-frequency oscillations of the estimated trajectories around the *true* trajectories.

These operational characteristics are mainly independent on the initiation of the filtering, but are highly dependent on the applied relative weighting for the residual errors and, in turn, on the applied constant gains. (The stabilized values of the time-varying diagonal gain equations depend on the applied relative weighting for the residual errors.)

In the investigated cases, the best tracking performance was obtained by the constant-gain diagonal filter. This filter can be mechanized by approximately 95% reduction of the mathematical operations needed to mechanize the corresponding full filter scheme. The IBM 7094 digital simulation time for the constant-gain diagonal filter is less than the simulated actual flight time. (Even for the time-varying diagonal filter the digital simulation time is less than the actual flight time in the investigated cases.) Thus, the developed simplified digital filters have a particularly fast working property which, in principle, makes them well suited for on-board mechanization.

The simplifications developed in the present study should primarily be viewed in relation to the particular application in question since, the problem being nonlinear, the application itself also enters into the analysis and design of the nonlinear filter. Nevertheless, the developed simplifications may be indicative for other particular problems as well.

Appendix A

System and Observation Equations

In deriving the equations of motion of a ballistic vehicle the following assumptions are made. The planet is spherical, nonrotating and its acceleration of gravity is constant. Furthermore, the distribution of the atmospheric density is inversely exponential with respect to the altitude, and the drag depends quadratically on the velocity and linearly on the atmospheric density. Then, in a trajectory-fixed reference frame and in a nonmoving atmosphere, the planar motion of the center of gravity of a nonlifting, gravity-turn ballistic vehicle in free fall is described by the following system of ordinary nonlinear differential equations (see also Fig. A-1):

$$\dot{x}_1 = -x_3 \sin x_2 \tag{A-1}$$

$$\dot{x}_2 = \left(\frac{g}{x_3} - \frac{x_3}{r}\right) \cos x_2 \tag{A-2}$$

$$\dot{x}_3 = g \sin x_2 - K x_3^2 \exp(-b x_1) \tag{A-3}$$

$$\dot{x}_4 = x_3 \cos x_2 \tag{A-4}$$

where the dot denotes the time derivative and

- x_1 $\triangleq$ altitude, positive, upward from the surface of the planet
- x_2 $\triangleq$ path angle, positive, below the local horizontal
- x_3 $\triangleq$ velocity, positive, downward
- x_4 $\triangleq$ ground range, relative to some reference vertical
- g $\triangleq$ acceleration of gravity
- r $\triangleq$ radius of the planet, $r \gg x_1$
- b $\triangleq$ inverse scale factor for the exponential distribution of the atmospheric density
- K $\triangleq$ drag parameter, reflecting the ballistic characteristics of the vehicle as well as the ground level pressure on the planet

In view of the assumptions specified above, Eqs. (A-1) through (A-4) describe the vehicle's motion at the terminal section of a soft-landing mission when $x_1 \leqq 10$ mi and $x_3 \leqq 700$ mi/h. The model for the atmospheric density distribution corresponds to an isothermal atmosphere in hydrostatic equilibrium. From the point of view of estimating the state of the vehicle in some time interval during the terminal phase of a soft-landing mission, Eqs. (A-1) through (A-4) can be regarded as the best available *a priori* physical knowledge on the motion of the vehicle in that period of time. The main uncertainty regarding the dynamic description of the vehicle's motion is due to the acting atmospheric forces. This dynamic uncertainty can be said to be reflected in the values of parameters K and b as well as in omitting the unknown wind and random atmospheric forces (turbulence, etc.) from the dynamic equations.

For a *linear* observation vector, the following simple relations are employed

$$\begin{bmatrix} y_1 \\ y_2 \\ y_3 \end{bmatrix} = \begin{bmatrix} h \\ \alpha \\ v \end{bmatrix} = \begin{bmatrix} \text{altitude} \\ \text{path angle} \\ \text{velocity} \end{bmatrix} = \begin{bmatrix} x_1 + \text{noise} \\ x_2 + \text{noise} \\ x_3 + \text{noise} \end{bmatrix} \tag{A-5}$$

The quantities y_1, y_2, y_3 can be thought to be the evaluated outputs of some proper measuring devices.

For a *nonlinear* observation vector, the following relations are applied (Fig. A-2):

$$\begin{bmatrix} y_1 \\ y_2 \\ y_3 \end{bmatrix} = \begin{bmatrix} d \\ W_X \\ W_Y \end{bmatrix} = \begin{bmatrix} \frac{1}{c} x_1 + \text{noise} \\ x_3 \sin(x_2 - \theta) + \text{noise} \\ x_3 \cos(x_2 - \theta) + \text{noise} \end{bmatrix} \tag{A-6}$$

where

- d $\triangleq$ slant range
- θ $\triangleq$ slant range angle
- c $\triangleq$ $\sin \theta$
- W_X $\triangleq$ velocity in the body-referenced X direction
- W_Y $\triangleq$ velocity in the body-referenced Y direction

The observation vector given by Eq. (A-6) corresponds to measurements provided by a body-mounted radar altimeter and by a body-mounted doppler radar velocity sensor for a planar motion (Ref. 13).

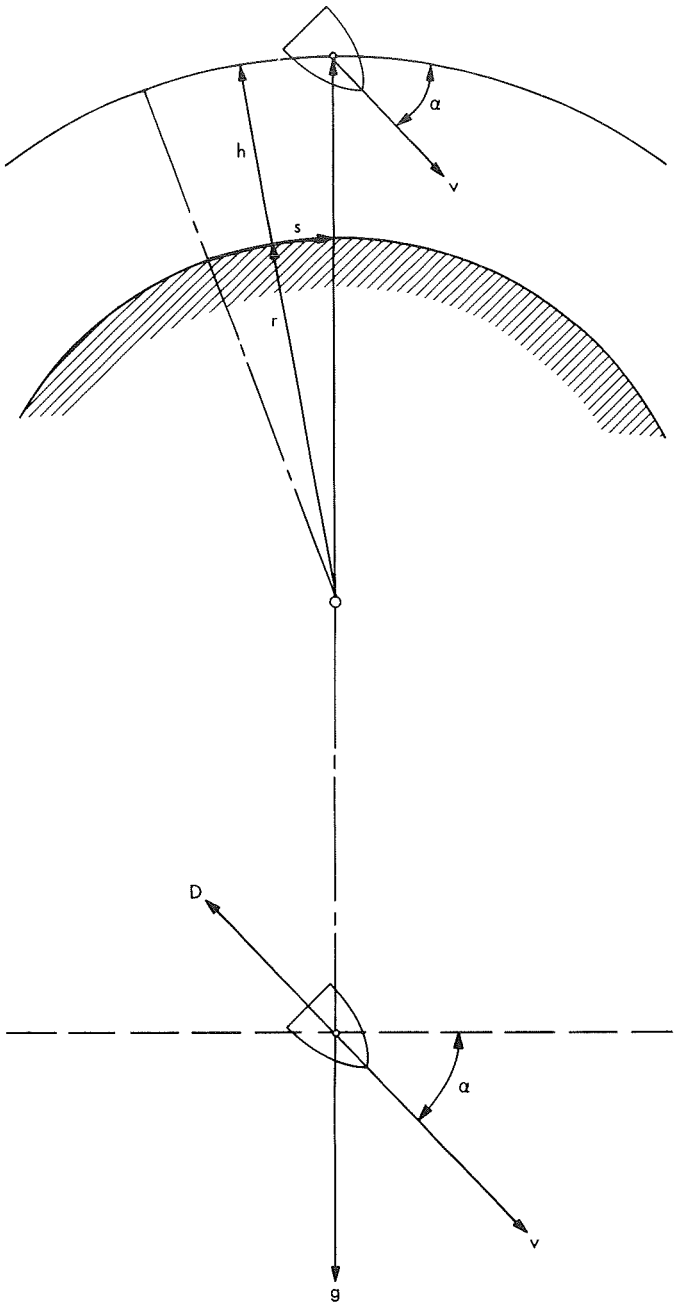

h = ALTITUDE
α = PATH ANGLE
v = VELOCITY
s = GROUND RANGE
D = DRAG
g = GRAVITY
r = RADIUS OF THE PLANET

Fig. A-1. State variables and forces

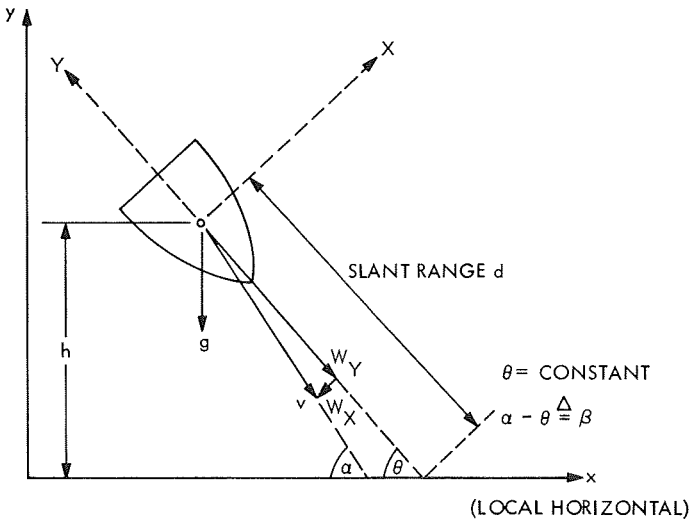

$$\text{MEASUREMENT VECTOR:} \quad \begin{pmatrix} d \\ W_X \\ W_Y \end{pmatrix} = \begin{pmatrix} \frac{h}{\sin\theta} + \text{NOISE} \\ v \sin\beta + \text{NOISE} \\ v \cos\beta + \text{NOISE} \end{pmatrix}$$

$$\text{STATE VECTOR:} \quad \begin{pmatrix} h \\ \beta \\ v \end{pmatrix} = \begin{pmatrix} D \sin\theta \\ \arctan \frac{W_X}{W_Y} \\ \left(W_X^2 + W_Y^2\right)^{1/2} \end{pmatrix}$$

Fig. A-2. A nonlinear measurement vector for ballistic descent

Appendix B

Full Nonlinear Filter Equations for the Linear Observation Vector

When the sequential estimation problem is restricted to estimating altitude x_1, path angle x_2, and velocity x_3, Eq. (A-4) in the system equations is not of interest since the ground range x_4 does not appear in the remaining differential equations governing the time histories of the altitude, path angle, and velocity. Thus, the dimensionality of the state vector x will be the same as of the linear observation vector y defined in Appendix A by Eq. (A-5). The Jacobian of that observation vector is

$$H = \begin{bmatrix} 1 & 0 & 0 \\ 0 & 1 & 0 \\ 0 & 0 & 1 \end{bmatrix} \tag{B-1}$$

For convenience, the identity matrix is selected for the quasi-norm factor Q related to the observations. Hence,

$$HQ\overline{H} = \begin{bmatrix} 1 & 0 & 0 \\ 0 & 1 & 0 \\ 0 & 0 & 1 \end{bmatrix} \tag{B-2}$$

The Jacobian of the system equations, Eqs. (A-1) through (A-3), is

$$F = \begin{bmatrix} 0 & -\hat{x}_3 \cos \hat{x}_2 & -\sin \hat{x}_2 \\ 0 & -\left(\frac{g}{\hat{x}_3} - \frac{\hat{x}_3}{r}\right) \sin \hat{x}_2 & -\left(\frac{g}{\hat{x}_3^2} + \frac{1}{r}\right) \cos \hat{x}_2 \\ bK\hat{x}_3^2 \exp(-b\hat{x}_1) & g \cos \hat{x}_2 & -2K\hat{x}_3 \exp(-b\hat{x}_1) \end{bmatrix} \tag{B-3}$$

Hence, the full maximum principle least-squares (MPLS) nonlinear filter schemes [Eqs. (1–3) in Section II-A] for sequentially estimating altitude, path angle, and velocity becomes:

$$\dot{\hat{x}}_1 = -\hat{x}_3 \sin \hat{x}_2 + 2P_{11}(y_1 - \hat{x}_1) + 2P_{12}(y_2 - \hat{x}_2) + 2P_{13}(y_3 - \hat{x}_3) \tag{B-4}$$

$$\dot{\hat{x}}_2 = \left(\frac{g}{\hat{x}_3} - \frac{\hat{x}_3}{r}\right) \cos \hat{x}_2 + 2P_{12}(y_1 - \hat{x}_1) + 2P_{22}(y_2 - \hat{x}_2) + 2P_{23}(y_3 - \hat{x}_3) \tag{B-5}$$

$$\dot{\hat{x}}_3 = g \sin \hat{x}_2 - K\hat{x}_3^2 \exp(-b\hat{x}_1) + 2P_{13}(y_1 - \hat{x}_1) + 2P_{23}(y_2 - \hat{x}_2) + 2P_{33}(y_3 - \hat{x}_3) \tag{B-6}$$

$$\dot{P}_{11} = -2(P_{11}^2 + P_{12}^2 + P_{13}^2) - 2(P_{12}\hat{x}_3 \cos \hat{x}_2 + P_{13} \sin \hat{x}_2) + R_{11} \tag{B-7}$$

$$\dot{P}_{12} = -2(P_{11}P_{12} + P_{12}P_{22} + P_{13}P_{23}) - \cos \hat{x}_2 \left[P_{22}\hat{x}_3 + P_{13}\left(\frac{g}{\hat{x}_3^2} + \frac{1}{r}\right)\right] - \sin \hat{x}_2 \left[P_{23} + P_{12}\left(\frac{g}{\hat{x}_3} - \frac{\hat{x}_3}{r}\right)\right] + R_{12} \tag{B-8}$$

$$\dot{P}_{13} = -2(P_{11}P_{13} + P_{12}P_{23} + P_{13}P_{33}) + \cos \hat{x}_2(gP_{12} - P_{23}\hat{x}_3) - P_{33} \sin \hat{x}_2 + K\hat{x}_3 \exp(-b\hat{x}_1) \cdot [bP_{11}\hat{x}_3 - 2P_{13}] + R_{13} \tag{B-9}$$

$$\dot{P}_{22} = -2(P_{12}^2 + P_{22}^2 + P_{23}^2) - 2P_{22}\sin\hat{x}_2\left(\frac{g}{\hat{x}_3} - \frac{\hat{x}_3}{r}\right) - 2P_{23}\cos\hat{x}_2\left(\frac{g}{\hat{x}_3^2} - \frac{1}{r}\right) + R_{22} \tag{B-10}$$

$$\dot{P}_{23} = -2(P_{12}P_{13} + P_{22}P_{23} + P_{23}P_{33}) + \cos\hat{x}_2\left[gP_{22} - P_{33}\left(\frac{g}{\hat{x}_3^2} + \frac{1}{r}\right)\right]$$
$$- P_{23}\sin\hat{x}_2\left(\frac{g}{\hat{x}_3} - \frac{\hat{x}_3}{r}\right) + K\hat{x}_3\exp(-b\hat{x}_1)\,[bP_{12}\hat{x}_3 - 2P_{23}] + R_{23} \tag{B-11}$$

$$\dot{P}_{33} = -2(P_{13}^2 + P_{23}^2 + P_{33}^2) + 2P_{13}bK\hat{x}_3^2\exp(-b\hat{x}_1) + 2P_{23}\,g\cos\hat{x}_2 - 4P_{33}K\hat{x}_3\exp(-b\hat{x}_1) + R_{33} \tag{B-12}$$

When $(1/r) \ll (g/\hat{x}_3^2)$, then $1/r$ can be omitted from the filter equations.

Appendix C

Full Nonlinear Filter Equations for the Nonlinear Observation Vector

It is assumed that the sequential estimation problem is restricted to estimating altitude, path angle, and velocity (the essential system variables from the point of view of the terminal guidance goal). Consequently, the fourth system equation [Eq. (A-4), Appendix A] is again not of interest since the differential equations for the altitude, path angle, and velocity are not dependent on the ground range. Thus, the dimensionality of the state vector x is the same as of the nonlinear observation vector y defined by Eq. (A-6) in Appendix A. The transpose of the Jacobian of that observation vector is

$$\bar{H} = \begin{bmatrix} \frac{1}{c} & 0 & 0 \\ 0 & \hat{x}_3 \cos(\hat{x}_2 - \theta) & -\hat{x}_3 \sin(\hat{x}_2 - \theta) \\ 0 & \sin(\hat{x}_2 - \theta) & \cos(\hat{x}_2 - \theta) \end{bmatrix} \tag{C-1}$$

For convenience, the identity matrix is selected again for the quasi-norm factor Q related to the observations. Hence, Eq. (3) in Section II-A becomes

$$g = 2 \begin{bmatrix} \frac{1}{c}\left(y_1 - \frac{1}{c}\hat{x}_1\right) \\ \hat{x}_3 [y_2 \cos(\hat{x}_2 - \theta) - y_3 \sin\hat{x}_2 - \theta)] \\ y_2 \sin(\hat{x}_2 - \theta) + y_3 \cos(\hat{x}_2 - \theta) - \hat{x}_3 \end{bmatrix} \tag{C-2}$$

The Jacobian of the vector g given by Eq. (C-2) is then

$$G = 2 \begin{bmatrix} -\frac{1}{c^2} & 0 & 0 \\ 0 & -\hat{x}_3 [y_2 \sin(\hat{x}_2 - \theta) + y_3 \cos(\hat{x}_2 - \theta)] & [y_2 \cos(\hat{x}_2 - \theta) - y_3 \sin(\hat{x}_2 - \theta)] \\ 0 & [y_2 \cos(\hat{x}_2 - \theta) - y_3 \sin(\hat{x}_2 - \theta)] & -1 \end{bmatrix} \tag{C-3}$$

The Jacobian of the system equations of Appendix A [Eqs. (A-1) through (A-3)] is the same as that of Eq. (B-3) in Appendix B. Hence, the full MPLS nonlinear filter scheme [Section II-A, Eqs. (1) and (2)] for sequentially estimating altitude, path angle, and velocity becomes in this case:

$$\begin{aligned} \dot{\hat{x}}_1 = & -\hat{x}_3 \sin\hat{x}_2 \\ & + 2P_{11}\frac{1}{c}\left(y_1 - \frac{1}{c}\hat{x}_1\right) \\ & + 2P_{12}\{\hat{x}_3 [y_2 \cos(\hat{x}_2 - \theta) - y_3 \sin(\hat{x}_2 - \theta)]\} \\ & + 2P_{13}[y_2 \sin(\hat{x}_2 - \theta) + y_3 \cos(\hat{x}_2 - \theta) - \hat{x}_3] \end{aligned} \tag{C-4}$$

$$\begin{aligned} \dot{\hat{x}}_2 = & \left(\frac{g}{\hat{x}_3} - \frac{\hat{x}_3}{r}\right)\cos\hat{x}_2 \\ & + 2P_{12}\frac{1}{c}\left(y_1 - \frac{1}{c}\hat{x}_1\right) \\ & + 2P_{22}\{\hat{x}_3 [y_2 \cos(\hat{x}_2 - \theta) - y_3 \sin(\hat{x}_2 - \theta)]\} \\ & + 2P_{23}[y_2 \sin(\hat{x}_2 - \theta) + y_3 \cos(\hat{x}_2 - \theta) - \hat{x}_3] \end{aligned} \tag{C-5}$$

$$\begin{aligned} \dot{\hat{x}}_3 = & g \sin\hat{x}_2 - K\hat{x}_3^2 \exp(-b\hat{x}_1) \\ & + 2P_{13}\frac{1}{c}\left(y_1 - \frac{1}{c}\hat{x}_1\right) \\ & + 2P_{23}\{\hat{x}_3 [y_2 \cos(\hat{x}_2 - \theta) - y_3 \sin(\hat{x}_2 - \theta)]\} \\ & + 2P_{33}[y_2 \sin(\hat{x}_2 - \theta) + y_3 \cos(\hat{x}_2 - \theta) - \hat{x}_3] \end{aligned} \tag{C-6}$$

$$\dot{P}_{11} = -2P_{12}\hat{\dot{x}}_3 \cos \hat{x}_2 - 2P_{13} \sin \hat{x}_2 - \frac{2}{c^2} P_{11}^2$$
$$- 2P_{12}^2 \hat{\dot{x}}_3 [y_2 \sin (\hat{x}_2 - \theta) + y_3 \cos (\hat{x}_2 - \theta)]$$
$$+ 4P_{12}P_{13} [y_2 \cos (\hat{x}_2 - \theta) - y_3 \sin (\hat{x}_2 - \theta)]$$
$$- 2P_{13}^2 + R_{11} \qquad \text{(C-7)}$$

$$\dot{P}_{12} = -P_{22}\hat{\dot{x}}_3 \cos \hat{x}_2 - P_{23} \sin \hat{x}_2 - P_{12}\left(\frac{g}{\hat{x}_3} - \frac{\hat{\dot{x}}_3}{r}\right) \sin \hat{x}_2$$
$$- P_{13}\left(\frac{g}{\hat{x}_3^2} + \frac{1}{r}\right) \cos \hat{x}_2 - \frac{2}{c^2} P_{11}P_{12}$$
$$- 2P_{12}P_{22}\hat{\dot{x}}_3 [y_2 \sin (\hat{x}_2 - \theta) + y_3 \cos (\hat{x}_2 - \theta)]$$
$$+ 2(P_{12}P_{23} + P_{13}P_{22}) [y_2 \cos (\hat{x}_2 - \theta)$$
$$- y_3 \sin (\hat{x}_2 - \theta)] - 2P_{13}P_{23} + R_{12} \qquad \text{(C-8)}$$

$$\dot{P}_{13} = -P_{23}\hat{\dot{x}}_3 \cos \hat{x}_2 - P_{33} \sin \hat{x}_2 + P_{11}Kb\hat{\dot{x}}_3^2 \exp (-b\hat{x}_1)$$
$$+ P_{12}g \cos \hat{x}_2 - 2P_{13}K\hat{\dot{x}}_3 \exp (-b\hat{x}_1) - \frac{2}{c^2} P_{11}P_{13}$$
$$- 2P_{12}P_{23}\hat{\dot{x}}_3 [y_2 \sin (\hat{x}_2 - \theta) + y_3 \cos (\hat{x}_2 - \theta)]$$
$$+ 2(P_{12}P_{33} + P_{13}P_{23}) [y_2 \cos (\hat{x}_2 - \theta)$$
$$- y_3 \sin (\hat{x}_2 - \theta)]$$
$$- 2P_{13}P_{33} + R_{13} \qquad \text{(C-9)}$$

$$\dot{P}_{22} = -2P_{22}\left(\frac{g}{\hat{x}_3} - \frac{\hat{\dot{x}}_3}{r}\right) \sin \hat{x}_2 - 2P_{23}\left(\frac{g}{\hat{x}_3^2} + \frac{1}{r}\right) \cos \hat{x}_2$$
$$- \frac{2}{c^2} P_{12}^2 - 2P_{22}^2 \hat{\dot{x}}_3 [y_2 \sin (\hat{x}_2 - \theta) + y_3 \cos (\hat{x}_2 - \theta)]$$
$$+ 4P_{22}P_{23} [y_2 \cos (\hat{x}_2 - \theta) - y_3 \sin (\hat{x}_2 - \theta)]$$
$$- 2P_{23}^2 + R_{22} \qquad \text{(C-10)}$$

$$\dot{P}_{23} = -P_{23}\left(\frac{g}{\hat{x}_3} - \frac{\hat{\dot{x}}_3}{r}\right) \sin \hat{x}_2 - P_{33}\left(\frac{g}{\hat{x}_3^2} + \frac{1}{r}\right) \cos \hat{x}_2$$
$$+ P_{11}Kb\hat{\dot{x}}_3^2 \exp (-b\hat{x}_1) + P_{12}g \cos \hat{x}_2$$
$$- 2P_{13}K\hat{\dot{x}}_3 \exp (-b\hat{x}_1) - \frac{2}{c^2} P_{12}P_{13}$$
$$- 2P_{22}P_{23}\hat{\dot{x}}_3 [y_2 \sin (\hat{x}_2 - \theta) + y_3 \cos (\hat{x}_2 - \theta)]$$
$$+ 2(P_{22}P_{33} + P_{23}^2) [y_2 \cos (\hat{x}_2 - \theta) - y_3 \sin (\hat{x}_2 - \theta)]$$
$$- 2P_{23}P_{33} + R_{23} \qquad \text{(C-11)}$$

$$\dot{P}_{33} = 2P_{13}Kb\hat{\dot{x}}_3^2 \exp (-b\hat{x}_1) + 2P_{23}g \cos \hat{x}_2$$
$$- 4P_{33}K\hat{\dot{x}}_3 \exp (-b\hat{x}_1) - \frac{2}{c^2} P_{13}^2$$
$$- 2P_{23}^2 \hat{\dot{x}}_3 [y_2 \sin (\hat{x}_2 - \theta) + y_3 \cos (\hat{x}_2 - \theta)]$$
$$+ 4P_{23}P_{33} [y_2 \cos (\hat{x}_2 - \theta) - y_3 \sin (\hat{x}_2 - \theta)]$$
$$- 2P_{33}^2 + R_{33} \qquad \text{(C-12)}$$

When $(1/r) \ll (g/\hat{x}_3^2)$, then $1/r$ can be omitted from the filter equations.

Appendix D

Applied Parameters and Computation Subroutines

The digital simulations were carried out on an IBM 7094 computer using a JPL-modified DSL/90 digital simulation language. The gaussian random numbers were generated by the DSL/90 functional subroutine called NORMAL. The uniformly distributed random numbers were generated by a JPL functional subroutine called PRN. The applied parameter values are as follows:

Mass of the vehicle: 31.1 slugs

Ballistic coefficient: 0.3 slug/ft^2

Mars gravity: 12.3 ft/s^2

Mars radius: 11.2×10^6 ft

Mars atmosphere, corresponding to the VM-7 model:

$\rho_0 = 1.32 \times 10^{-5}$ slugs/ft^3, ground level density

$b = 2.15 \times 10^{-5}$ ft^{-1}, inverse scale factor

Hence, the value of parameter K is:

$$K = \frac{1}{2} \cdot \frac{1}{0.3} \cdot 1.32 \times 10^{-5}$$

$$= 2.20 \times 10^{-5}\ \text{ft}^{-1}$$

Nomenclature

b inverse scale factor for the exponential distribution of atmospheric density

c sin θ; θ = slant range angle

g acceleration of gravity

K drag parameter, reflecting the ballistic characteristics of the vehicle as well as the ground level pressure on the planet

r radius of the planet

x_1 altitude

x_2 path angle

x_3 velocity

y_1 measured altitude

y_2 measured body-referenced velocity component when nonlinear observations are employed; measured path angle when linear observations are employed

y_3 measured body-referenced velocity component when nonlinear observations are employed; measured velocity when linear observations are employed

(P_{ij}) gain matrix

(Q_{ij}) weighting matrix, related to the measurements

(R_{ij}) weighting matrix, related to the system equations

Superscripts

$\cdot$ time derivative

$\wedge$ estimated values

$-$ compensated values for R; or the transpose of matrixes H and F

$*$ constant values for the gains

References

1. Kalman, R. E., "New Methods in Wiener Filtering Theory," in *First Symposium on Engineering Applications of Random Function Theory and Probability, 1963.* Edited by J. L. Bogdanoff and F. Kozin. John Wiley & Sons, Inc., New York, 1963.

2. Smith, G. L., "Multivariable Linear Filter Theory Applied to Space Vehicle Guidance," *J. Soc. Ind. Appl. Math.,* Vol. 2, No. 1, pp. 19–32, Jan. 1964.

3. Cox, H., "Estimation of State Variables via Dynamic Programming," paper presented at the Fifth Joint Automatic Control Conference, Stanford University, Palo Alto, Calif., 1964.

4. Detchmendy, D. M., and Sridhar, R., "Sequential Estimation of States and Parameters in Noisy Nonlinear Dynamical Systems," *J. Basic Eng.,* Vol. 88, Series D, No. 2, pp. 362–369, 1966.

5. Bass, R. W., Norum, V. D., and Schwartz, L., "Optimal Multichannel Nonlinear Filtering," *J. Math. Anal. Appl.,* Vol. 16, pp. 152–164, Oct. 1966.

6. Schwartz, L., and Stear, E. B., "A Valid Mathematical Model for Approximate Nonlinear Minimal Variance Filtering," *J. Math. Anal. Appl.,* Vol. 21, pp. 1–6, 1968.

7. Jazwinski, A. H., "Filtering for Nonlinear Dynamical Systems," *IEEE Trans. Automat. Cont.,* Vol. AC-11, pp. 765 and 766, 1966.

8. Bucy, R. S., "Nonlinear Filtering Theory," *IEEE Trans. Automat. Cont.,* Vol. AC-10, p. 198, 1965.

9. Friedland, B., and Bernstein, J., "Estimation of the State of a Nonlinear Process in the Presence of Nongaussian Noise and Disturbances," *J. Franklin Inst.,* Vol. 281, No. 6, pp. 455–480, 1966.

10. Schwartz, L., and Stear, E. B., "A Computational Comparison of Several Nonlinear Filters," *IEEE Trans. Automat. Cont.,* Vol. AC-13, pp. 83–86, 1968.

11. Kushner, H. J., "Approximations to Optimal Nonlinear Filters," *IEEE Trans. Automat. Cont.,* Vol. AC-12, pp. 546–556, 1967.

12. Bejczy, A. K., "On the Realization and Computational Aspects of the Maximum Principle Least-Squares Nonlinear Filter," in *Proceedings of the Second Hawaii International Conference on System Sciences,* University of Hawaii, Honolulu, Hawaii, pp. 365–368, 1969.

13. Pfeffer, J., "Terminal Guidance for Soft Lunar Landing," in *Guidance and Control of Aerospace Vehicles.* Edited by C. T. Leondes. McGraw-Hill Book Co., Inc., New York, 1963.

NASA — JPL — Coml., L.A., Calif.